In contrast to the above, Levresse et al. (1997) found that chrysotile and crocidolite act to inhibit proliferation in cultured rat pleural mesothelioma (RPM) cells. In this study, RPM cells (diploid, no more than 25 passages) were dosed with either UICC crocidolite or NIEHS Zimbabwean Chrysotile at concentrations varying between 0.5 and 20 $\mu g/cm^2$. The authors also note that the chrysotile sample contains approximately 4 times the number of fibers as the crocidolite samples. Cells were then examined at 4, 24, and 48 hours following treatment. In untreated cultures, the number of cells in replicative phase decrease with time, which indicates that such cells are headed for confluence (completion of a monolayer on the culture medium). At 48 hours, for example, 10% of untreated control cells were observed to be in replicative stage. Chrysotile (but not crocidolite) decreased the fraction of cells in replicative phase in a time- and dose-dependent manner. At 48 hours, for example, cells treated with 10 $\mu g/cm^2$ chrysotile showed only 1.5% in replicative phase. Further tests confirmed that this was due to blockage of cells at the G1/S boundary of the cell cycle. Both chrysotile and crocidolite appears to induce a time-dependent increase in the number of cells at G2/M in the cell cycle, although this effect was not observed to be dose-dependent for chrysotile. Even on a fiber-number basis, chrysotile appears to be elicit a greater response (arrest a greater percentage of cells) than crocidolite.

The authors also indicate that chrysotile caused nuclear-localized, time-dependent increases in p53 concentrations. Crocidolite produced much lower levels that were not detectable in the nucleus. Chrysotile was also observed to produce blockage at the G0/G1 transition of the cell cycle, but crocidolite did not. They also note that p53 is known to mediate arrest at this stage in the cycle so observing that chrysotile induces arrest at this transition in the cell cycle may be consistent with the observed increased expression of p53. The authors also note that chrysotile triggers apoptosis in this study and that crocidolite shows a smaller, but detectable effect. Spontaneous apoptosis in untreated cultures ran between 0.5 and 1% at 24–48 hours whereas chrysotile induced 4% apoptosis, peaking at 72 hours following exposure to 10 $\mu g/cm^2$. The authors indicate that the lower level of effects observed with crocidolite could be due to the substantially smaller number of long fibers in UICC crocidolite compared to NIEHS chrysotile.

The previously reviewed (Section 6.3.3.1) study by Hart et al. (1994) also suggests that long, medium, short, and UICC crocidolite and chrysotile along with a range of MMVF's show a dose-dependent inhibition on proliferation of cultured CHO cells and that potency toward the effect is a direct function of fiber length.

Several of the above-described studies, in addition to providing evidence that asbestos induces proliferation in various lung tissues, also suggests certain mechanisms. Asbestos may induce proliferation, for example, by inducing production of specific cytokine growth factors (Adamson 1997; Brody et al. 1997), or by inducing certain signaling cascades (Barchowsky et al. 1997, Timblin et al. 1998b). It is also possible that the two effects may be related (i.e., that stimulation of a particular signaling cascade may result in production of certain growth-stimulating cytokines). Other mechanisms may also be important (Table 6-5).

6.3.4.2 Asbestos induced cell signaling

Asbestos has been shown to induce a variety of cell signaling cascades in a variety of target cell and tissue types. Such signaling may then trigger effects in the stimulated cells that may include:

- proliferation;
- morphological changes;
- generation and release of various cytokines, enzymes, or extracellular matrix; or
- programmed cell death.

Note, due to the large number of chemical species that need to be considered in this discussion, Table 6-6 provides a summary of the sources of such species (Table 6-6A) and the effects attributable to such species (Table 6-6B).

In specific cases, asbestos may initiate cell signaling by interacting directly with receptors on the cell surface, by causing generation and release of intermediate species (e.g., ROS or RNS) that trigger cell signaling, or (for phagocytized fibers) by interacting with intracellular components of a particular signaling cascade. The specific responses to cell signaling induced by asbestos are frequently cell- or tissue-type specific. Moreover, depending on the specific mechanism, cell signaling by asbestos may be dependent on fiber size and/or type.

Barchowsky et al. (1998) showed in a set of studies that long chrysotile and long crocidolite, but not RCF-1 fibers (at concentrations between 1 and 10 $\mu g/cm^2$), which is reportedly below levels that typically induce cytotoxic effects) induced up-regulation of urokinase-type plasminogen activator (uPA) and its receptor (uPAR) in both lung endothelial cells (vascular cells) and lung epithelial cells. They also showed that the increased pericellular protolytic activity (requiring cleavage of plasminogen to plasmin) that is induced by asbestos in these cells is mediated by uPA.

In prior studies, chrysotile has been shown to cause endothelial cells to elongate and increase expression of adhesion molecules for phagocytes. They also show enhanced proteolytic activity and matrix interactions. Chrysotile has also been shown to stimulate fibrinolytic activity in lung epithelial cells and extravasating macrophages. All such stimulation appears to result from up-regulation of uPA. Thus, this mechanism may explain the observed asbestos-induced changes in lung endothelial and epithelial cells including vascular remodeling, development of vascularized granular tissue, increased matrix turnover, and leukocyte extravasation (which in turn may be caused by cell activation and elaboration of proteases and adhesion molecules). The authors suggest that asbestos-induced up-regulation of uPA and uPAR expression may represent a global mechanism for pulmonary toxicity and fibrosis induced by crystalline fibers. Importantly, chrysotile was shown to induce uPA and uPAR expression in the absence of serum, so the effect is apparently due to direct binding of fibers to cell-surface receptors.

Mossman et al. (1997) observed that concentrations of 1.25–5 $\mu g/cm^2$ of crodidolite (sample from TIMA) caused expression of c-jun and AP-1 in both cultured hamster tracheal epithelial (THE) cells and cultured rat pleural mesothelial (RPM) cells. Crocidolite was also observed to trigger the EGFR-regulated kinase (ERK) and mitogen activated protein kinase (MAPK) pathways in RPM cells. The authors indicate that these pathways are also stimulated by hydrogen peroxide and that NF-$\kappa\beta$ induction stimulated by crocidolite is also stimulated by crystalline silica (although silica stimulation of the MAPK pathway was not investigated). They also note that the non-fibrous analog to crocidolite, riebeckite does not elicit these activities.

The authors indicate that induction of the NF-$\kappa\beta$ cascade was inhibited by excess glutathione, which is stimulated by N-acetylcysteine (NAC), suggesting that this pathway is induced by asbestos-caused oxidative stress (perhaps through ROS or RNS intermediates). Application of NAC also diminished crocidolite induced c-fos and c-jun RNA levels and inhibited activation of the ERK-MAPK cascade. Further work suggests that asbestos triggers the MAPK pathway by interaction with the Epithelial Growth Factor Receptor (EGFR), either directly or by phosphorylation of this receptor by ROS. At the concentrations examined, crocidolite induces substantial apoptosis (apparently through activation of the ERK-MAPK cascade). In contrast, the authors note that TNF-α induces the JNK arm of the ERK-MAPK cascade, which leads to proliferation. Asbestos does not elevate JNK over the time-period of the study. The authors note that it has been shown in some studies that inhibition of ERK in some cells, also inhibits asbestos-induced apoptosis. Importantly, given that these processes are induced by crocidolite, but not by its non-fibrous analog, riebeckite, induction of the ERK-MAPK cascade appears to be a fiber-size dependent process.

In a related study to that conducted by Mossman et al. (1997), Zanella et al. (1999) report that the (TIMA) crocidolite (at concentrations of 2.5–10 μg/cm^2, but not its non-fibrous analog, riebeckite, eliminated binding of EGF to its receptor EGFR. Because EGF does not bind to crocidolite in the absence of membrane, this is not simply a case of crocidolite tying up ligand. Crocidolite also induces a greater than 2-fold increase in steady-state message and protein levels of EGFR.

The authors also note that the tyrphostin, AG-1478 (which specifically inhibits the tyrosine kinase activity of EGFR), significantly mitigated asbestos-induced increases in mRNA levels of c-fos, but not c-jun, and that the asbestos action was not blocked by a non-specific tyrphostin, AG-10. Moreover, pretreatment of RPM cells with AG1478 significantly reduced asbestos-induced apoptosis. Therefore, the authors concluded that asbestos-induced binding to EGFR initiates signaling pathways responsible for increased expression of the protooncogene c-fos and the development of apoptosis. This apparently occurs through the EGFR-extracellular signaling regulated kinase (ERK). It is hypothesized that asbestos may induce dimerization and activation (phosphorylation) of EGFR, which also prevents binding of EGF. Asbestos apparently serves the same role as EGF in that it promotes aggregation of EGFR, which in turn promotes binding to the extracellular domain of tyrosine kinase receptors and the activation of their intracellular kinases. The authors also indicate that other work suggests that crocidolite fiber exposure leads to aggregation and accumulation of EGFR at sites of fiber contact and that asbestos also stimulates biosynthesis of the EGFR and activates ERK in an EGFR-dependent manner.

The authors speculate that asbestos binding may not be ligand-site specific, but may be charge related or may induce EGFR phosphorylation by local production of ROS, which has previously been demonstrated to cause EGFR activation. As previously indicated, that this effect is driven by crocidolite exposure, but not by exposure to riebeckite indicates that this mechanism is fiber-size specific.

Johnson and Jaramillo (1997) showed that UICC crocidolite, but not JM-100 glass, applied to a culture of immortalized human Type II epithelial (A549) cells at non-cytotoxic concentrations (for 20 hours) results in increased expression of p53, Cip1, and GADD153 in a dose- and time-dependent fashion. Expression was observed to be maximum at 18 hours. The crocidolite treatment was also shown to cause an increase in the number of cells arrested in Stage G2 of the cell cycle (with a persistent decrease in the number of cells in G1). This was considered surprising because both p53 and Cip1 are known to mediate arrest in Stage G1. The authors suggest that these findings indicate a strong dependence on both fiber type and fiber size (JM-100 glass contains substantially more long fibers than crocidolite). However, it is not possible to separate the effects of fiber type versus fiber size in this study.

Luster and Simeonova (1998) indicate that at high concentrations, ROS may induce frank cytotoxicity. At low or moderate levels, ROS are more likely to induce cell signaling cascades that may, in turn, contribute to asbestos-related disease. The authors dosed cultures of immortalized human Type II epithelial (A549) cells, originally derived from a lung carcinoma, and normal human bronchioepithelial (NHBE) cells with long (Certain-Teed supplied) crocidolite (reported mean length: 19 μm) at concentrations ranging between 0 and 24 μg/ml. Results indicate that secretion of both Interluken-8 (IL-8) and IL-6 was stimulated by crocidolite exposure in a dose-dependent manner. In contrast, increases in LDH levels (which indicate cell damage) was only detected at the highest exposure concentrations tested. Further work indicates that stimulation of IL-6 and IL-8 secretion occurs through ROS that are generated in an iron-dependent process (that may also include NF-κβ induction). Note that the trend of cell signal induction at low and moderate levels of asbestos exposure with evidence for cytotoxicity observed only at the highest exposure concentrations is common to many of these kinds of studies.

Choe et al. (1999) conducted a combined *in vivo/in vitro* study of the effects of low level exposure to chrysotile or crocidolite at inducing leukocyte attachment to rat pleural mesothelial cells. The authors note that similar populations of rat pleural leukocytes (74% macrophages, 2% neutrophils, 10% mast cells, and 10% eosinophils) were observed in both asbestos-exposed and unexposed rats.

In the second part of the study, cultured RPM cells were exposed to either crocidolite or chrysotile (both NIEHS samples) at concentrations ranging between 1.25 and 10 $\mu g/cm^2$, which was noted to be below levels at which substantial cytotoxicity is observed. Attachment of rat pleural leukocytes to RPM cells was then observed to increase with increasing dose of asbestos to the RPM cells. In contrast, carbonyl iron (a non-fibrous particle) also induced enhanced attachment, but at much lower levels and the effect was not dose-dependent. Further analysis indicated that asbestos-induced adhesion is mediated by up-regulation of IL-1β (but not dependent on TNF-α or nitric oxide production, although it is noted that TNF-α independently increases attachment). Asbestos also induces increased expression of vascular cell adhesion molecule (VCAM-1). The authors also note that rat pleural leukocytes harvested from asbestos-exposed rats also showed increased adhesion to *in vitro* RPM cells over leukocytes harvested from sham exposed rats. Thus, asbestos appears to trigger alterations in these cells as well.

In a recent paper, Driscoll et al. (1997) reviewed the role of tumor necrosis factor alpha (TNF-α) in mediating the inflammatory response to lung insult by particulate matter. The authors indicate that quartz, coal dust, crocidolite, and chrysotile are all potent inducers of TNF-α production. Titanium dioxide (TiO_2), corundum (aluminum oxide: Al_2O_3), and latex beads are not. Pulmonary macrophages have been shown to secrete TNF-α *in vivo* in response to exposure to some of the dusts listed above (including asbestos). This is also observed among macrophages from asbestosis patients.

The authors indicate that rats immunized against TNF-α show reduced recruitment of neutrophils, which demonstrates that TNF-α is involved in the recruitment of inflammatory cells. TNF-α stimulates macrophages, epithelial cells, endothelial cells, and fibroblasts to release chemokines that include adhesion molecules (Eselectin, ICAM, VCAM). Inflammatory cells then interact with such molecules and migrate along gradients from vascular structures in the lung to the lung interstitium and even the lung air spaces. It has also been shown that release of TNF-α by macrophages is apparently dependent on oxygen stress (i.e., exposure to ROS/RNS) that is induced in pathways that require iron. Production of TNF-α and other compounds that mediate the inflammatory response are regulated by the oxidant-sensitive transcription factor NF-$\kappa\beta$. This factor exists as a heterodimer in the cytoplasm in an inactive form because it is bound to the inhibitory 1-kappaBalpha (1-$\kappa B\alpha$), which masks a nuclear translocation signal. Appropriate stimulation of a cell induces phosphorylation of 1-$\kappa B\alpha$, which then marks it for proteolytic degradation. Then, NF-$\kappa\beta$ translocates to the nucleus and induces transcription. The process is stimulated by oxidants and inhibited by antioxidants.

In another review, Finkelstein et al. (1997) indicated that Type II epithelial cells and Clara cells (non-ciliated bronchiolar epithelial cells) respond to and produce specific cytokines during the inflammatory process. Early responses to particle challenge include increases in mRNA and protein for IL-1β, IL-6, and TNF-α. These are also accompanied by changes in specific epithelial genes including those for surfactant protein C and Clara cell secretory protein. The authors further indicate that these responses are due to direct interaction with particles rather than a result of macrophage-derived mediators and they suggest a more significant role for epithelial secretions in the overall pulmonary response than previously suspected. Results also suggest that Type II pneumocyte-derived growth factors may play a significant role in the pathogenesis of pulmonary fibrosis.

Also in this paper, Finkelstein et al. (1997) report that intratracheal instillation of lipopolysaccharide (a potent inflammatory agent) caused increases in both lavage fluid and plasma levels of TNF-α and IL-6. Intrapleural injection induced primarily increases in plasma levels. The authors indicate that this suggests that the observed cytokines are produced primarily at the site of injury. The authors further indicate that

IL-6 is elevated in lavage fluids following exposure to Ni_2S_3, a suspected human carcinogen, but not following exposure to TiO_2 or NiO. *In vitro* studies indicate that release of IL-1β and TNF-α by Type II cells occurred only following exposure to crocidolite or ultrafine TiO_2, but not pigment grade TiO_2. The authors also indicate that protein C and Clara cell secretory protein were both expressed in their respective source cells following exposure only to the fibrogenic of the above particles. They also report that crystalline silica has been shown to promote cytokine release and hypertrophy in Type II cells.

Jagirdar et al. (1997) used immunohistochemistry in a study to show that all three isoforms of TGF-β (1,2, and 3) are expressed in the fibrotic lesions of asbestosis and pleural fibrosis patients from the Quebec mines, primarily by Type II pneumocytes. The cases examined averaged 38 years of exposure to the Quebec chrysotile. The authors also indicate that the hyperplastic epithelium of silicosis patients also show elevated expression of all three isoforms. They further indicate from previous studies that mesothelioma tumor cells frequently express TGF-β2 while the cells in the stroma of such tumors frequently express TGF-β1. It is also noted in this study that jun and fos are both transcription factors that activate the TGF-β1 promoter.

Zhang et al. (1993) indicate that macrophages obtained in BAL fluid from idiopathic pulmonary fibrosis (IPF) patients and asbestosis patients show significantly increased secretion of TNF-α and asbestosis patients also showed significantly increased secretion of IL-1β. Macrophages and monocytes obtained from both kinds of patients also show elevated expression of mRNA for these cytokines. In an *in vitro* part of this study, Zhang and coworkers, showed that chrysotile, crocidolite, amosite, and crystalline silica all stimulated IL-1β and TNF-α release and up-regulated their respective mRNA in both macrophages and monocytes. The authors also report that these two cytokines have been shown to up-regulate collagen Types I and III and fibronectin gene expression in human diploid lung fibroblasts after short-term, serum free exposure *in vitro*.

Holian et al. (1997) exposed cultures of normal human alveolar macrophages (AM) (obtained by lavage) to varying concentrations (up to 25 μg/ml) of short chrysotile, UICC crocidolite, ground silica, wollastonite, and titanium dioxide to determine whether these materials cause a phenotypic shift in macrophage populations by inducing selective apoptosis. The authors indicate that normal lungs contain: 40–50% RFD1+7+ suppressor AM, and 5–10% RFD1+ immune activator. In this study, the fibrogenic subset of the particles tested (not wollastonite or titanium dioxide) increased the ratio of activator/suppressor AM by a factor of 4 within a few hours and the effect was seen to increase with time. The authors also note that fibrogenic particles decrease the abundance of RFD7+ AM (phagocytic), but the consequences of this phenotypic shift are unclear.

The authors indicate that AM taken from fibrotic patients release a variety of proinflammatory mediators capable of stimulating fibroblast proliferation and collagen synthesis. Even in the absence of evidence of fibrosis, workers who have been heavily exposed to asbestos yield similarly activated AM. In contrast, they also note that, *in vitro* studies in which AM are stimulated with fibrogenic particles, while such AM are activated to release inflammatory cytokines, such releases are orders of magnitude less than that seen from AM derived from fibrotic patients. The authors indicate that the apoptosis-driven phenotypic shift in AM that is indicated by this study may explain the apparent discrepancy.

In a previously described study, Timblin et al. (1998a), see Section 6.3.4.1, showed that crocidolite asbestos and several cation substituted erionites all stimulate c-jun and c-fos in rat pleural mesothelial cells, but to varying degrees depending on fiber chemistry. The effect also appears to be size dependent as crocidolite, but not its non-fibrous analog riebeckite induces the effect.

In general, the kinds of signaling cascades that are potentially stimulated by exposure to asbestos are important due to their potential to contribute to the promotion of cancer. Such pathways, for example, may mediate proliferation or may suppress apoptosis. Alternately, they may mediate an inflammatory

response that in turn may lead to proliferation or to production and release of other, mutagenic agents (e.g., ROS or RNS). Pathways that facilitate development of fibrosis may also contribute to cancer promotion, given the apparent link between fibrosis and the development of lung cancer, which may relate (among other possibilities) to inhibition of fiber clearance (Section 6.3.4.5).

The ERK-MAPK signaling pathway evaluated in multiple studies by Mossman and coworkers (Mossman et al. 1997; Timblin et al. 1998a,b; Zanella et al. 1999) in rat pleural mesothelial (RPM) cells is a case in point (see above). These studies suggest that crocidolite stimulates the ERK-MAPK cascade through interaction with the EGF receptor. This ultimately leads to transcription of mRNA for c-fos. Crocidolite has also been shown to induce c-jun (apparently through a separate mechanism) and the balance between c-jun and c-fos has been implicated in guiding a cell toward either proliferation or apoptosis. Although the direct connection between c-jun/c-fos and apoptosis has not been established, it is observed that crocidolite induces substantial apoptosis in RPM cells at the same concentrations at which it induces substantial expression of c-fos and c-jun. The link is also implied because inhibition of the ERK pathway has been shown in some studies to inhibit asbestos-induced apoptosis. Na-erionite has also been shown to induce c-fos at levels comparable or higher than crocidolite for comparable exposures (at least on a mass basis) and induce c-jun at higher levels. However, it is not known whether Na-erionite and crocidolite act via the same pathways. Potentially due to the increased, relative expression of c-jun induced by Na-erioinite, increased apoptosis is not observed in association with exposure to Na-erionite. However, the link between increased c-jun expression and inhibition of apoptosis has not been demonstrated explicitly.

Both crocidolite and Na-erionite were also shown by Mossman and coworkers to induce uptake of bromodeoxyuridine (BrdU) by RPM cells in these same experiments. Uptake of BrdU is an indicator of DNA synthesis. Since it has also been shown that crocidolite is capable of damaging DNA via ROS and other pathways (Sections 6.3.3) and both crocidolite and erionite are known to induce mesotheliomas in any case, the balance between proliferation and apoptosis in this cell population that is struck by exposure to these toxins may very well determine whether development of cancers are promoted or prevented. Of course, both proliferation and apoptosis may also be mediated by other pathways independent of the ones described here.

The problem is that the range of responses that are induced by asbestos in the lung are varied and complex (see Table 6-5) so that it has not yet been possible to definitively identify the biochemical triggers that lead to lung cancer or mesothelioma. It is even likely, for example, that different mechanisms (or combinations of mechanisms) predominate under different exposure conditions or in association with differing fiber types or particle sizes. Still, examination of the dependence of candidate mechanisms on fiber type and particle size can be instructive, especially to the degree that such indications are consistent with observations in whole animal studies (see, for example, Section 6.2.2). For the signaling cascade described above by Mossman and coworkers, for example, the effects attributable to crocidolite are clearly dependent on fiber size because the non-fibrous analog to crocidolite, riebeckite does not induce any of the effects. It also appears that the chemistry of the fibers is important, given the observed differences in responses among the various, substituted erionites.

6.3.4.3 Asbestos-induced apoptosis

Apoptosis (programmed cell death) is generally triggered when a cell accumulates certain types of genetic damage, when cell signaling cascades are triggered by external stimuli that may occur, for example, as part of the need to maintain tissue homeostasis or to cause a phenotypic shift in response to toxic challenge (see, for example, Holian et al. 1997, Section 6.3.4.2), or when a cell has completed a pre-programmed number of divisions. Asbestos can induce apoptosis in a variety of cells by several mechanisms including primarily:

- by causing sufficient genetic damage to trigger apoptosis; or
- by triggering a signal cascade that leads to apoptosis.

As previously indicated, asbestos may trigger signaling cascades by interacting directly with receptors on the cell surface, or by inducing production of intermediate species (such as ROS or RNS) that may in turn induce cell signaling.

Some of the mechanisms by which asbestos may act to induce apoptosis may be fiber size- or type-dependent. Also, responses may vary in different target tissues.

Fibers. As indicated in Section 6.4.3.2, crocidolite (but not the non-fibrous analog riebeckite) induces apoptosis in hamster tracheal epithelial cells and rat pleural mesothelial cells when applied at non-cytotoxic concentrations (Mossman et al. 1997). Results from the study also indicate that apoptosis is triggered in this case by inducing an ERK-MAPK signaling cascade as a consequence of interaction with EGF receptors on the cell surface. The interaction may be direct or may be caused by asbestos-induced ROS. In a related study (also previously summarized, Section 6.3.4.1), Timblin et al. (1998a) indicate that the asbestos-induced apoptosis reported in the Mossman et al. (1997) work is fiber-type specific and the pathway involved appears to stimulate expression of c-fos.

In a study previously reported in greater detail (Section 6.3.4.1), Levresse et al. (1997) indicate that chrysotile induces apoptosis in cultured rat pleural mesothelioma cells with the effect peaking at 4% at 72 hours following exposure to 10 $\mu g/cm^2$. Although the authors observed a much smaller effect with crocidolite, they indicate that the difference is likely due to the much smaller number of long fibers in the particular crocidolite sample evaluated.

Broaddus et al. (1997) indicates that crocidolite (not UICC), but not wollastonite, glass beads, or non-fibrous riebeckite cause substantial apoptosis in rabbit pleural mesothelioma cells in culture in a dose-dependent fashion. The extent of apoptosis induced was inhibited by treatment with catalase and by 3-minobenzamide (an inhibitor of poly(ADP-ribosyl) polymerase. The former indicates a role for ROS mediation and the latter indicates that this enzyme, which mediates DNA repair, also mediates asbestos-induced apoptosis (perhaps triggered by asbestos-induced DNA damage). Asbestos induced apoptosis was also inhibited by treatment with desfeoxamine, but effects were restored by adding iron to the medium. The authors note that in other studies, crocidolite has been shown to induce DNA strand breaks within 2 hours after exposure and induces unscheduled DNA synthesis within 24 hours following exposure. Asbestos also induces production of poly(ADP-ribosyl) polymerase.

Non-fibrous particles. Leigh et al. (1997) intratracheally instilled rats with silica (a non-fibrous particle) at doses varying between 2 and 22 mg. They then collected cells by bronchio-alveolar lavage (BAL) 10 days after instillation. The authors observed large numbers of apoptotic cells in BAL fluid and that the number of such cells was dose-dependent. The dead cells were primarily neutrophils (so that this might represent some type of mechanism to restore homeostasis). Engulfment of apoptotic cells by macrophages was also observed. The authors report that, 56 days after instillation, apoptotic cells were observed in granulomatous tissue within the lungs of rats exposed to silica. This suggests that apoptosis may also occur in response to chronic inflammation. The authors conclude that silica induces apoptosis among granulomatous cells and alveolar cells and that such apoptosis and the subsequent engulfment of apoptotic cells by macrophages may play a role in the evolution of silica-related disease. The authors also note that granuloma formation is a hyperplasia-related event.

At least some of the mechanisms suggested above for asbestos-induced apoptosis are dependent on fiber size (the non-fibrous analog of crocidolite does not induce the effect) and dependent on the chemistry of the fibers involved (various, cation-substituted analogs of erionite exhibit disparate ability to induce the

effect). Although non-fibrous particles (such as crystalline silica) may also induce apoptosis, as previously suggested, this may be through separate mechanisms from those responsible for asbestos-related effects, even if the same endpoint results.

6.3.4.4 Asbestos-induced cytotoxicity

While there is ample evidence from various *in vitro* studies that asbestos is cytotoxic, such effects are observed almost exclusively at the highest concentrations evaluated in an experiment (for example, Luster and Simeonova [1998], Section 6.3.4.2 and Choe et al. [1999], Section 6.3.4.2). Many experiments are conducted at concentrations below those for which cytotoxicity is important because the other toxic effects attributable to asbestos occur at substantially lower exposure levels and researchers prefer to study such effects in the absence of potentially confounding cytotoxicity. For *in vitro* studies, for example, non-cyotoxic effects are typically studied at concentrations less than approximately 10 $\mu g/cm^2$ (or 20 $\mu g/ml$) while substantial cytotoxicity is not typically observed until exposure concentrations are several times higher.

Because most of the other effects attributable to asbestos occur at concentrations that are substantially lower, this begs the question as to whether frank cytotoxicity is an effect that is relevant to human exposures. There is also substantial evidence that the mechanisms associated with asbestos-induced cytotoxicity are separate from the mechanisms that mediate most of the other asbestos-related effects of interest.

Kamp et al. (1993) dosed cultured pulmonary epithelial (PE) cells with UICC amosite asbestos. In some studies, polymorphonuclear leukocytes (PMN) were also added to the culture. Typical doses in this experiment were on the order of 250 $\mu g/cm^2$, which is quite high for these types of studies. For example, compare this level with the levels reported for studies of ROS/RNS generation (Section 6.3.3), cell signaling (Section 6.3.4.2), proliferation (Section 6.3.4.1) or apoptosis (Section 6.3.4.3).

Kamp and coworkers indicate that the effect of amosite exposure on cultured PE cells (at the concentrations studied) was to induce substantial cell lysis (cytotoxicity) and little cell detachment (from the culture medium), which would indicate increased cell motility. Addition of PMN to the culture resulted in both increased cell lysis and cell detachment for comparable exposures to amosite. The observed cell detachment was mitigated in a dose-dependent fashion by adding protease inhibitors. Further work indicated that asbestos induces release of human neutrophil elastase (HNE), which may mediate the combined effects with PMN. PE cell exposure to HNE alone causes increases in cell detachment in a dose-dependent fashion. However, when combined with asbestos exposure, cell lysis increases at the expense of cell detachment. The authors suggest that HNE becomes bound to asbestos, which also becomes bound to PE cells and this facilitates augmented cytotoxicity by proteases that are secreted by PMN's.

Blake et al. (1998) studied the effect of fiber size on the cytotoxicity of alveolar macrophages *in vitro*. Cultured cells were dosed with concentrations varying between 0 and 500 $\mu g/ml$ of each of 5 different length preparations of JM 100 glass fiber. Cytotoxicity was monitored by assays for extracellular LDH and by chemiluminescence following zymosan addition. The latter assy is intended to show macrophage stimulation. Results indicate that all samples showed dose-dependent increases in toxicity (i.e., increasing LDH and decreasing chemiluminescence). Comparing across samples, relatively long fibers (mean=17 μm) showed the greatest toxicity. The authors further indicate that microscopic examination suggests that frustrated phagocytosis plays a role in cytotoxicity.

Goodglick and Kane (1990) studied the effect of three different length preparations of crocidolite (long, short, and UICC) on elicited macrophages (stimulated initially with thioglycolate) *in vitro* and *in vivo*.

The long and short samples were reportedly prepared from the UICC sample by repeated centrifugation. Goodglick and Kane (1990) report that all three types of crocidolite stimulated release of ROS from macrophages. At sufficiently high concentrations, all three also caused substantial cytotoxicity, although apparently due to the longer time required to settle in culture, the full effects from short fibers take longer to develop. They suggest that, on a total fiber number or surface area basis, long and short crocidolite appear to exhibit approximately equal potency toward the cytotoxicity of macrophages. Further work with various inhibitors indicates that cytotoxicity is mediated by production of ROS and that ROS are produced via an iron-dependent pathway. They also indicate that, among the effects of crocidolite exposure is that macrophage mitochondrial membranes are depolarized.

Goodglick and Kane (1990) also evaluated the effects of long and short crocidolite *in vivo*. This was done by evaluating the effects of intraperitoneal injection of the various samples (long, short, or mixed crocidolite or titanium dioxide particles) in C57B1/6 mice. Results indicate that a single injection of long crocidolite (480 μg) induced an intense inflammatory response, leakage of albumin, and fibers observed scattered across the diaphragm. In contrast, a single injection of short crocidolite (600 μg) induced only a relatively mild inflammatory response and only limited clusters of fibers observed on the surface of the diaphragm.

To test whether short fibers would show a greater response, if they were not cleared more readily than long fibers, Goodglick and Kane (1990) also subjected mice to 5 consecutive, daily injections of 120 μg of short crocidolite and noted more substantial aggregations of fiber clusters along the diaphragm as well as a more pronounced inflammatory response. Cell injury was also assessed by Trypan blue staining (which indicates cell death). All mice singly or multiply injected with mixed or long crocidolite showed marked Trypan blue staining. Single injections of short structures showed only limited Trypan blue staining. However, following 5 daily injections of short fibers, multiple Trypan blue stained cells were observed on the diaphragm in the vicinity of the locations were clusters of fibers were also observed. The authors also indicate (in contrast) that neither single injections of 160 or 800 μg nor 5 consecutive (160 μg) injections of titanium dioxide produced any Trypan blue staining.

The authors conclude from this study that both short and long crocidolite fibers appear to be cytotoxic to macrophages while titanium dioxide particles are not (suggesting that not only fiber length, but fiber type is important to cytotoxicity). They further suggest that, while short fibers tend to be cleared rapidly *in vivo*, when such clearance mechanisms are overwhelmed (such as by repeated insult through repeated, daily injections in this study), then the toxic effects of short structures becomes apparent. As indicated in other studies, however, there may be multiple mechanisms working to produce similar responses, that such mechanisms may exhibit varying dose-response characteristics, and that cytotoxicity may not generally be directly related to mechanisms that contribute to carcinogenesis. Moreover, there almost certainly are at least some longer fibers in the short fiber preparation and extended analysis to determine their relative concentration with adequate precision would be helpful to see if the relative magnitude of the observed effects correlate.

Palekar et al. (1979) studied the ability of four different samples of commingtonite-grunerite, each also subjected to varying degrees of grinding, to induce hemolysis of mammalian erythrocytes and cytotoxicity to Chinese hamster ovary (CHO) cells. The samples studied include: UICC amosite (4.13 m^2/g surface area/mass), which is denoted as "asbestiform grunerite; "semi-asbestiform" commingtonite (3.88 m^2/g); acicular commingtonite (ground to three particle sizes: 3.76, 2.45, and 0.82 m^2/g), and acicular grunerite (2.82 m^2/g).

Results from this study indicate that amosite induced the greatest hemolysis of erythrocytes by far (approximately 50%) while acicular, unground grunerite caused no hemolysis. However, grinding the acicular grunerite to increasingly smaller particle sizes and greater surface area ultimately results in some hemolysis. Both semi-asbestiform and acicular, unground commingtonite show hemolytic activity

between amosite and unground, acicular grunerite and grinding acicular commingtonite also increased its hemolytic activity.

Similar results were also observed for cytotoxicity. Amosite was by far the most cytotoxic and the effect was dose-dependent. A dose of 0.05 mg/ml caused approximately 75% cell death for CHO cells. At 0.2 mg/ml, only 1% of cells survived. Acicular grunerite was nontoxic even at 0.5 mg/ml. With grinding, acicular grunerite cytotoxicity increased, albeit only slowly. The most heavily ground sample killed fewer than 25% of cells at 0.2 mg/ml and killed only 65% at 0.5 mg/ml. The cytotoxicity of semi-asbestiform commingtonite was substantially less than amosite, but greater even than ground, acicular grunerite. For this material, 0.2 mg/ml killed approximately 65% of cells and 0.5 mg/ml killed approximately 90%. Interestingly, approximately the same dose-response curve for cytotoxicity was observed for the 3.88 and 1.61 specific surface area samples of this material. The 1.21 samples was somewhat less cytotoxic. Acicular commingtonite was somewhat less cytotoxic (for corresponding doses) than semiasbestiform commingtonite at the highest specific surface area (3.76) and its toxicity decreased with decreasing surface area.

The authors also indicate that neither surface charges on crystal particles nor Magnesium ion content appear to correlate with biological activity. The authors conclude that the degree of "asbestiform" character of a mineral has a dominant effect on biological activity. Moreover, although non-fibrous particles may also be biologically active (and their activity increases with increasing specific surface area), the effects of particles and fibers lie along entirely separate dose-response curves. The biological activity of fibrous materials does not appear to depend directly on specific surface area.

Importantly, the results of the Palekar et al. (1979) study are also consistent with the possibility that fibrous structures within a specific range of sizes and shapes contribute strongly to biological activity while largely non-fibrous particles act through a separate mechanism that depends primarily on total surface area, but that particle-for-particle elicits a substantially lower overall response than the mechanism by which fibers act. Such a scenario is supported by several studies. Jaurand (1997), for example, indicate that ROS are implicated in the cytotoxicity of long, but not short fibers on tracheal epithelial cells. Although the evidence for distinct mechanisms for fibers and particles discussed here is specific to cytotoxic and hemolytic effects, evidence in other studies suggest similar scenarios for other toxic endpoints (potentially including endpoints that contribute to carcinogenicity).

Comparisons of the rate and extent of effects observed in epidemiology studies, whole animal dose-response studies, and *in vitro* studies suggests that cytotoxicity may not be important to human exposures. Unfortunately, however, there is currently insufficient information to compare doses and exposures across these studies in a more quantitative fashion. Therefore, the importance of cytotoxicity to human asbestos exposure cannot be definitively determined at this time.

6.3.4.5 Association between fibrosis and carcinogenicity

The hypothesis that lung tumor induction is associated with the fibrosis has been examined by several authors. There appears to be a debate as to whether fibrosis is a necessary precursor for development of lung cancer (associated with exposure to fibers), whether the presence of fibrosis is an additional factor contributing to increased risk for lung cancer, or whether the two diseases are largely unrelated. This is an important consideration because the characteristics of the exposure-response relationship between asbestos and lung cancer or asbestosis (fibrosis) apparently differ (Sections 6.3.6 and 6.4).

Based on animal studies, Davis and Cowie (1990) found that rats that developed pulmonary tumors during inhalation experiments exhibited a significantly greater clinical degree of fibrosis than rats that did not develop tumors. Furthermore, Davis and Cowie (1990) reported suggestive evidence that the

pulmonary tumors that did develop in the dosed rats tended to develop within portions of the rat's lungs that were already scarred by fibrosis.

As part of a review, Mossman and Churg (1998) indicate that fibrosis of any cause (including diffuse idiopathic fibrosis) appears to be associated with an increased risk of lung cancer and that this is observed in both human and animal studies. They also indicate that only those strains of mice and hamsters that develop fibrotic lesions following exposure to crystalline silica show an increased risk of developing cancer. They also report that, in parallel to what is reported for asbestos by Davis and Cowie (1990), lung tumors that develop following exposure to crystalline silica tend to occur primarily (if not exclusively) in those portions of the lung where fibrotic lesions predominate.

In contrast, Case and Dufresne (1997) from their study of lung burdens among Quebec miners and millers indicate that there is high overlap in the range of concentrations that lead to both lung cancer and asbestosis and those that lead to lung cancer alone, which the authors suggest show a lack of relationship between the two diseases (one is not predictive of the other). The authors indicate that, based on regression of the 111 cases they examined, the only indicator that reasonably tracks lung cancer is severity of smoking and they indicate that this is true despite the level of fiber content in the lung.

Although a definitive determination concerning the relationship between fibrosis (asbestosis) and lung cancer cannot be developed at this time, it does appear that there is some association between the two diseases. Most likely, fibrosis is an additional risk factor for lung cancer and thus represents an additional set of mechanisms that may contribute to the overall risk of developing lung cancer in association with exposure to asbestos. However, based on the evidence as a whole, including the evidence that the character of the dose-response relationship for lung cancer and asbestosis differ, it is not clear that development of fibrosis is an absolute precursor that is required before asbestos-related lung tumors can develop. Interestingly, based on the studies reviewed by Mossman and Churg (1998), the relationship between fibrosis and lung cancer induced by silica may be substantially stronger than that between fibrosis and lung cancer induced by asbestos.

6.3.4.6 Interaction between asbestos and smoking

Numerous studies have indicated a synergistic relationship between smoking and asbestos exposure toward the induction of lung cancer (see, for example, Hammond et al. 1979; Kamp et al. 1992, 1998; Mossman et al. 1996). Smoking is also suspected to facilitate development of asbestos-induced fibrosis (Kamp et al. 1992). However, a more recent study (Liddell and Armstrong 2002) suggests a more complicated relationship that is closer to additive than multiplicative (for a more detailed discussion of this study, see Section 7.2.3). Therefore, discussion of a more complex interaction (which may not be specifically synergistic) is addressed below.

Putative mechanisms that may contribute to an interaction between asbestos exposure and smoking include:

- facilitated transport of carcinogenic components of smoke that may be adsorbed on the surface of asbestos fibers, which may then serve as vehicles to transport these materials through cell membranes to cell interiors and even to locations adjacent to or within the nucleus (see, for example, Fubini 1997; Mossman et al. 1996);

- asbestos-catalyzed production of more highly mutagenic metabolites of the various components of smoke, including benzo(a)pyrene (see, for example, Mossman et al. 1996);

- smoke-product induced inhibition of clearance of asbestos fibers and/or asbestos induced inhibition of clearance of smoke products (see, for example, Mossman et al. 1996); and

- smoke-product induced facilitation of uptake of asbestos by lung epithelium (see, for example, Mossman et al. 1996).

Although much progress has been made at elucidating the nature of these mechanisms and other candidate mechanisms, at this point in time it is possible to indicate definitively neither what mechanisms are important to any observed interaction between smoking and asbestos exposure nor to indicate the relative magnitude of the contributions from such mechanisms. Moreover, a detailed review of such mechanisms is beyond the scope of this document.

6.3.4.7 Conclusions concerning asbestos as a promoter

There is strong evidence that asbestos acts as a promoter for cancer. While this may primarily involve mechanisms the contribute to the induction of proliferation, mechanisms associated with the an interaction between smoking and exposure to asbestos (for the induction of lung cancer; smoking does not appear to affect mesothelioma) are also important. There also appears to be an association between the development of fibrosis and an increased risk for lung cancer.

Evidence indicates that multiple mechanisms may be involved with asbestos-induced cancer promotion and that such mechanisms may be complex and interacting. The different mechanisms also appear to exhibit dose-response relationships with differing characteristics. While there are indications that the most important among these mechanisms may be strong functions of fiber size (with long fibers contributing most to the induction of disease), mechanisms that depend primarily on surface area or total fiber (particle) number (for any size range) may also contribute to overall cancer promotion. Importantly, these latter mechanisms also appear to be strongly associated with the composition of fibers (particles) and may therefore contribute more substantially to the disease induction of agents that have been shown to be particularly toxic (such as crystalline silica), as opposed to particles, fibers, or asbestos in general.

At this point in time, the available data may not be sufficient to distinguish among the relative contributions from the various mechanisms to the overall promotion of cancer, at least in terms of the mechanistic data itself. Importantly, however, the mechanistic data should not be considered to be inconsistent with the results from whole animal studies, where there are clearer indications that fiber size plays a major role in carcinogenicity and fiber (particle) type is also important (see Sections 6.2 and 6.4). Such studies indicate, for asbestos (and other biodurable fibers) that:

- short fibers (less than somewhere between 5 and 10 μm) do not appear to contribute to disease;

- potency likely increases regularly for fibers between 10 μm and a minimum of 20 μm (and, perhaps, continues to increase up to lengths of at least 40 μm); and

- fiber type may be important primarily in determining biodurability.

They further indicate that particularly (or uniquely) toxic particles (such as crystalline silica) may act through a different set of mechanisms that are not dependent on fiber length, but that induce toxic endpoints paralleling those observed for asbestos.

Importantly, the mechanisms by which asbestos may act as a promoter appear to occur in cell lines that may contribute both to the induction of lung cancer and mesothelioma.

6.3.5 Evidence that Asbestos Induces an Inflammatory Response

There is ample evidence that asbestos induces an inflammatory response in pulmonary tissues and the pleura (see, for example, Sections 6.2.2 and 6.3). Moreover, there appears to be multiple biochemical triggers that mediate this response and various mechanisms may be fiber size- and/or fiber type-specific (Table 6-5). Because the role that inflammation plays in the induction of cancer has been addressed elsewhere (Sections 6.3.3 and 6.3.4), it is beyond the scope of this document to provide a detailed review of the mechanisms that lead specifically to inflammation.

6.3.6 Evidence that Asbestos Induces Fibrosis

There is ample evidence that asbestos induces fibrosis in pulmonary tissues (see, for example, Sections 6.2.2 and 6.3). Moreover, there appears to be multiple biochemical triggers that mediate this response and various mechanisms may be fiber size- and/or fiber type-specific (Table 6-5). Because the role that fibrosis plays in the induction of cancer has been addressed elsewhere (Sections 6.3.3 and 6.3.4), it is beyond the scope of this document to provide a detailed review of the mechanisms that lead specifically to fibrosis. Such mechanisms have also been the subject of recent reviews (see, for example, Mossman and Churg 1998; Robledo and Mossman 1999).

6.3.7 Evidence that Asbestos Mediates Changes in Epithelial Permeability

As previously indicated (Section 4.4), maintaining the overall integrity of the epithelial surface of the lung is among the various functions of Type II epithelial cells (Leikauf and Driscoll 1993). It has been shown that asbestos induces changes in the morphology of Type II epithelial cells (see, for example, Ilgren and Chatfield 1998), which has the effect (among others) of increasing the overall permeability of lung epithelial tissue to various macromolecules and, potentially to asbestos fibers themselves. The former plays a role in asbestos-induced fibrosis (by allowing cytokines that stimulate fibroblast proliferation or stimulate fibroblasts to generate extracellular matrix to pass through the epithelium and reach the underlying fibroblasts, Section 6.3.6). The latter may be important to facilitating transport of asbestos from the alveolar lumen to the interstitium (see, for example, Lippmann 1994).

Changes in epithelial permeability may be triggered by cytokines released from other cells or by the action of asbestos fibers on epithelial cells directly. Moreover, some of the mechanisms that mediate this response may be sensitive to fiber size and/or fiber type. For example, Gross et al. (1994) showed that monolayers of human bronchial epithelial cells cultured over a porous medium and exposed to cryogenically ground chrysotile (average length: 1 μm, average aspect ratio:14 at 15 μg/culture plate) became permeable to fibrin breakdown products (FBP's). The cultures were grown over human serum with labeled fibrinogen. This was based on observed increased concentrations of FBP's (double in 24 hours) in the ablumenal chambers of exposed cells compared to cells in control cultures. Because the epithelium showed greater permeability to all concentrations, the increased concentrations were not due to increased breakdown. The observed FDP flux was not vectoral, not saturable, and required neither proteolytic processing nor active transport. Thus, asbestos increases the paracellular flux of intact FDP across airway epithelium.

6.3.8 Conclusions Regarding the Biochemical Mechanisms of Asbestos-Related Diseases

That the specific biochemical triggers for asbestos-related diseases (particularly, the asbestos-related cancers) have not been definitively delineated as of yet is not surprising. The detailed interactions between fibers (and particles) and the cells and tissues of the lung are complex and there are complex, multiple, interacting mechanisms by which such interactions may contribute to disease. Despite great progress in elucidating candidate mechanisms, the number of candidate mechanisms is large and

distinguishing among their relative contributions has been difficult. This is because, among other things, the ability to compare results across studies of different mechanisms is currently limited due to the inability to reconcile the quantitative effects of dose and response across dissimilar studies.

Nevertheless, a number of important implications can be gleaned from the available literature. First, it appears that asbestos can function both as a cancer initiator and a promoter. It also appears that both the initiation and promotion of cancer may occur through more than one mechanism.

Regarding cancer initiation, asbestos likely acts primarily through a mechanism involving interference with mitosis. By this mechanism, asbestos fibers are phagocytized by target cells, migrate to perinuclear locations, and interact with the spindle apparatus and other cell assemblages required to complete mitosis. This tends to result in aneuploidy and may cause various clastogenic effects. This mechanism is driven by long fibers; short fibers do not appear to contribute to the effect. It also appears that all asbestos fiber types (and potentially other durable fibers with sufficient dimensions) cause genetic damage via this mechanisms. If there are effects due to fiber type, they appear only to play a secondary role.

Although there is also evidence that asbestos may induce production of DNA adducts and DNA strand breaks (through ROS and RNS mediated pathways), whether such adducts or breaks ultimately lead to permanent, heritable changes to DNA remain to be demonstrated. The relative importance of ROS/RNS mediated pathways for initiating cancer, compared to the pathway involving interference with mitosis, also remains to be determined.

There is also some evidence that the relative importance of asbestos as a cancer initiator may differ in different tissues. Lung epithelial cells, for example, appear to be relatively resistant to the mechanisms by which asbestos may initiate cancer. Mesothelial cells are not. Among several possibilities, this may be due to the ability of proliferation-competent lung epithelial cells (Type II cells) to undergo terminal differentiation when challenged with certain toxins and this is a pathway not available to mesothelial cells.

The mechanisms by which asbestos may promote cancer primarily involve mechanisms that contribute to the induction of proliferation, although mechanisms associated with an interaction between smoking and exposure to asbestos to induce lung cancer are also important. There also appears to be an association between the development of fibrosis (including asbestosis) and an increased risk of lung cancer.

Evidence indicates that multiple mechanisms may be involved with asbestos-induced cancer promotion and that such mechanisms may be complex and interacting. The different mechanisms also appear to exhibit dose-response relationships with differing characteristics. While there are indications that the most important of these may be strong functions of fiber size (with long fibers contributing the most to carcinogenicity), mechanisms that depend primarily on surface area or total fiber number (for any size range) may also contribute to overall cancer promotion. These latter mechanisms also appear to be strongly associated with the composition of fibers and may therefore contribute more substantially to the disease induction of agents that have been shown to be particularly toxic, as opposed to particles, fibers, or asbestos in general.

Although crystalline silica may act to produce some of the same effects as asbestos (including carcinogenicity), there is substantial evidence that this family of materials do not act through the same pathways and that the characteristics of their respective dose-response relationships may differ. Thus, for example, while asbestos likely induces cancer through mechanisms that favor long (and potentially thin) fibers, silica more likely acts through a mechanism that is dependent on total surface area, with freshly and finely ground material likely being the most potent. In contrast, grinding asbestos fibers tends to lesson its carcinogenicity overall. Due to differences in chemistry and crystallinity (reinforced by studies indicating a lack of correspondence in behavior), crystalline silica does not appear to be an appropriate

analog for any of the asbestos fiber types. Rather, for example, the appropriate non-fibrous analog for crocidolite is riebeckite and the appropriate non-fibrous analog for chrysotile is antigorite or lizardite.

6.4 ANIMAL DOSE RESPONSE STUDIES

Ideally, human epidemiology studies (reviewed in Chapter 7) provide the best data from which to judge the effects of asbestos in humans and from which to derive exposure-response factors for humans. However, animal dose-response studies have proven useful for elucidating certain features of the relationship between asbestos dose and response that cannot be adequately explored in the human studies, primarily due to limitations in the manner that exposures were characterized in the human studies (see Chapter 5).

Unlike human epidemiology studies, exposures in animal studies are controlled and better quantified. Frequently, the characteristics (in terms of fiber size, shape, and type) of such exposures have also been better quantified and this has allowed exploration of the effects that such characteristics (fiber size, shape, type) have on disease response. Accordingly, an overview of animal dose-response studies is provided in this section. Both injection-implantation studies and inhalation studies are reviewed. Particular attention is also focused on a "supplemental" animal inhalation study that we conducted with the specific aim of identifying the characteristics of asbestos that best relate to risk. The strengths and limitations of these kinds of studies are described in Chapter 5.

6.4.1 Injection-Implantation Studies

Because the fibrous materials in injection and implantation studies are placed immediately against the target tissue, the effects of processes associated with inhalation, retention, and translocation are avoided. The only active mechanisms that need to be considered in these studies are those that occur directly in the target tissue (including degradation, clearance, and biological responses of the types described in the previous sections of this chapter). Fibrous materials placed against the tissue surface are subject to dissolution, phagocytosis by macrophages, and phagocytosis by the cells of the target tissue. These mechanisms are described in greater detail in Section 6.2. A range of biologic responses have also been observed (described in Section 6.3).

Numerous researchers have performed these types of studies.

The Work of Stanton and Coworkers. In a series of studies, Stanton and coworkers (1972, 1977, 1981) implanted fibrous materials and induced mesotheliomas in rats. In the studies, a pledgette composed of coarse glass is loaded with hardened gelatin containing sample material and is surgically implanted immediately against the left pleura of the rats. Control studies demonstrate that the coarse glass of the pledgette does not induce significant tumors in the absence of other tumorigenic agents in the gelatin.

Although the mass dose of material implanted was the same for all experiments (40 mg), the observed incidence of mesothelioma varied among samples. By characterizing the dimensions of fibrous structures in the samples using a microscope, the researchers were able to explore the relationship between fiber size and the incidence of mesothelioma. By studying a wide range of fibrous materials, Stanton and his coworkers concluded that the induction of mesothelioma is determined primarily by the physical dimensions of fibers and that mineral composition is secondary. Further, potency appears to increase with the length and decrease with the diameter of fibrous structures. The researchers also concluded that the incidence of malignant tumors correlates with the degree of fibrosis induced by the presence of the fibrous materials. This does not necessarily imply, however, that fibrosis is a necessary step in the induction of asbestos-induced tumors (see Section 6.3.4.5).

Conclusions from the Stanton et al. (1972, 1977, 1981) studies indicating that mineralogy is not a factor in biological response conflicts with evidence provided in Chapter 7 and implications gleaned from mechanism studies presented in Section 6.3. However, the studies by Stanton and coworkers have been shown to suffer from certain methodological limitations (Berman et al. 1995) so that results from these studies should be considered more qualitative than quantitative.

Due to limitations in the ability to produce samples composed of uniform fibers, quantitative relationships between size and potency were explored by Stanton and coworkers using a regression analysis. Structures longer than 8 μm with diameters less than 0.25 μm or longer structures with diameters less than 1.5 μm were found to represent the range of sizes that best correlate with carcinogenicity. It was further stated that such correlations did not eliminate the possibility that other size ranges also contribute to potency, only that the two size ranges identified appear to correlate best. Samples that varied significantly from the reported correlations were attributed to errors in the characterization of structure size distributions in those samples. However, other methodological limitations might also have contributed to the observed deviations or such "outliers" may also suggest evidence for a mineralogical effect that is similar to what is reported in other studies (see Section 6.3 and Berman et al. 1995).

The precision of estimates for the ranges of sizes that contribute to biological activity that are derived from the Stanton and coworkers (1972, 1977, 1981) studies is limited so that such estimates should also be considered qualitative. Size distributions were determined by characterizing 200 to 1,000 structures using TEM and there is no indication that statistically balanced counting rules were employed (Section 4.3). Under such conditions, counts of structures longer than 8 μm are likely small and subject to large uncertainties for most of the samples characterized. Confidence intervals are not provided for any of the exposure values presented in these studies.

Potentially larger errors in the studies by Stanton and coworkers could have been introduced by the method employed to relate fiber counts to sample mass. As indicated in Chapter 5, estimating contributions to mass by sizing total particles and assuming that this is proportional to total sample mass is subject to error from the limit to the precision of characterizing structure dimensions (particularly diameter) and by not accounting for nonasbestos (and possibly nonfibrous) material in the samples. Thus, for example, there is no discussion of the precision with which the cut point of 8 μm was determined in these studies.

Re-analysis and Extension of the Stanton Studies. Several researchers have re-evaluated data from the implantation studies to test additional hypotheses. Using the Stanton and coworkers (1972, 1977, 1981) data, Bertrand and Pezerat (1980) examined the relationship between mesothelioma incidence and several characteristics not evaluated by Stanton and coworkers including: average fiber length, average fiber diameter, average fiber aspect ratio, total fiber surface area and total fiber volume. Results from the regression analysis indicate that potency varies directly with average length and inversely with average diameter, but that neither parameter is a good indicator alone. Combining the effects of length and diameter, average aspect ratio is highly correlated with potency. Biological activity does not correlate highly with structure count, surface area or volume except when fiber sizes are restricted to the long, thin structures that Stanton and coworkers defined. Results of this study are not inconsistent with those originally presented by Stanton and coworkers except that they emphasize a set of characteristics that relate parametrically to biological activity rather than expressing exposure as a single restricted size range of structures.

Bertrand and Pezerat (1980) were able to find good correlations between response and specific "average" characteristics of the samples that are not proportional to the quantity of the material present in the sample ("intensive" characteristics). Such intensive characteristics as average aspect ratio, average length, or average diameter are properties that are independent of the mass of material in a sample. Since response

must be a function of the quantity of sample present, intensive characteristics should have to be multiplied by characteristics that are proportional to the mass of a sample (e.g., fiber number, sample mass, or sample volume) in order to relate them to response. Properties that vary with the mass of a sample are termed "extensive" properties.

The correlations between intensive properties and response reported by Bertrand and Pezerat (1980) likely succeed within the Stanton and coworkers (1972, 1977, 1981) database because a constant sample mass (40 mg) was employed for all of the implantation experiments. However, to apply dose-response relationships that are dependent only on intensive characteristics beyond the data presented by Stanton and coworkers (where mass dose will not be constant), it is necessary to pair intensive characteristics with extensive characteristics (such as mass or number of fibers per sample). Therefore, it is unclear how the conclusions from this paper may be generalized to other data sets.

In a similar study, Bonneau et al. (1986) also examined parametric relationships between structure characteristics and mesothelioma induction. The paper examined specifically correlations between carcinogenicity and dose in terms of two specific relationships: dose expressed as fibers longer than 8 μm that are thinner than 0.25 μm ("Stanton" fibers) and dose expressed as mean aspect ratio. The researchers conclude that mean aspect ratio provides an excellent indication of carcinogenicity for individual fiber types, but that each fiber type must be treated separately. Poorer correlations are found for the relationship between the concentration of "Stanton" fibers and mesothelioma, even when fiber types are considered independently. Although these results appear to be consistent with findings reported from mechanistic studies (Sections 6.2 and 6.3) in that they posit a role for fiber mineralogy, the relationships evaluated by Bonneau et al. (1986) also suffer from the limitation of expressing dose only in terms of intensive quantities, as discussed above. Direct comparison with other studies is therefore difficult.

Following up on the reported problems of the studies by Stanton and coworkers in characterizing crocidolite, Wylie et al. (1987) reanalyzed seven crocidolite samples originally studied by Stanton et al. She and coworkers then used the new size distributions to reevaluate the "Stanton hypothesis" (that the concentration of "Stanton" fibers in a sample correlates with carcinogenicity). Wylie and coworkers note that substantial deviations from the Stanton hypothesis occur for specific samples. They conclude that a specific structure size range alone is not sufficient to characterize biological activity and that a parametric relationship with other structure characteristics (potentially including mineral type) may be necessary to sufficiently describe biological activity.

Conclusions from the Wylie et al. (1987) paper must be interpreted carefully because the researchers evaluated only the relationship between carcinogenicity and the single specific size range indicated ("Stanton" fibers). Thus, the possibility that improved correlations exist between biological activity and different size ranges or a combination of size ranges cannot be ruled out. Qualitatively, conclusions presented in this paper are not inconsistent with the conclusions reported by Stanton and coworkers regarding the general relationship between response and fiber dimensions.

The Wylie et al. (1987) study appears to suffer from several methodological problems. These relate to the manner in which the sample reanalysis was performed. The drop method for preparing electron microscopy grids (used in this study) is not satisfactory for preparing grids. In fact, as reported in the study itself, grids prepared as duplicates by this method were shown to be non-uniform at the 95% confidence interval using a chi-square test. In addition, only 100 to 300 fibers were counted for each sample. Since there is no indication that statistically balanced counting was performed, the uncertainty associated with counts of "Stanton" fibers may be substantial. Such errors would be further multiplied by uncertainty introduced during the sizing of total particles to determine the number of fibers per unit mass.

In a later study, Wylie et al. (1993) examined the effect of width on fiber potency. In this latter study, results from animal injection and implantation studies were pooled and subjected to regression analyses to

identify correlations between exposure and tumor incidence. The animal studies selected for inclusion in this analysis were performed on a variety of tremolite samples exhibiting a range of morphological and dimensional characteristics.

In their regression analyses, Wylie et al. (1993) evaluated a range of exposure indices that emphasize different morphological or size characteristics to help elucidate the characteristics of asbestos that induce a biological response. Because all of the animal studies included in their analyses involved tremolite, mineralogy was not an issue. Results from this study suggest that fibers longer than 5 μm and thinner than 1 μm best correlate with tumor incidence among the animal injection and implantation studies examined. Further, they suggest that a width limit, rather than a limit on aspect ratio, better reflects the bounds of the asbestos characteristics that determine biological activity. They also suggest that complex structures (bundles and clusters) need to be evaluated as part of the determination of exposure because such structures can breakdown and contribute to the population of thinner fibers.

Although the results of the Wylie et al. study tend to support the general conclusions in this document related to width, if not to length (see Section 6.5 and Appendix A), as the authors themselves indicate, such results should be considered qualitative due to the limitations imposed on their study by the methodology employed. Their study was conducted by:

- combining results from multiple studies without careful consideration of variation introduced by methodological differences across the studies;
- employing asbestos concentrations determined by SEM and without careful consideration of differences in the counting methodologies employed by differing research groups across studies; and
- considering injection and implantation studies, which do not account for mechanisms related to inhalation and deposition that affect the exposure-response relationship in humans.

The limitations imposed by the above constraints are highlighted in Chapters 4 and 5 of this report.

Other Injection Studies. A series of injection studies were conducted by several research groups. In these studies, fibrous materials were suspended in saline and injected into rats immediately adjacent either to the pleura or peritoneum. A large number of fibrous materials have now been studied by this process, as reported by: Bolton et al. (1982, 1984, 1986); Davis et al. (1985, 1986a,d, 1987, 1988a); Muhle et al. (1987); Pott et al. (1974, 1976, 1978, 1982, 1987); and Wagner et al. (1976, 1982, 1985). Newer studies are also discussed in Section 6.2. Results confirm that it is the fibrous nature of the materials that is the primary factor leading to the induction of tumors and that potency appears to depend directly on length and inversely on diameter.

The authors of these studies tend to indicate that, except where fibers are not persistent *in vivo*, due to solubility or other degradation processes, the mineralogy of the fibers appears to play only a secondary role in determining disease incidence. Researchers conducting injection experiments also tended to report a correlation between tumor incidence and the degree of fibrosis induced by the sample. These observations are consistent with the ideas originally articulated by Stanton.

Pott developed Stanton's ideas further by suggesting that carcinogenicity is a continuous function of fiber dimensions, which decreases rapidly for lengths less than 10 μm and also decreases with increasing diameter. The possibility was also raised that the apparent inverse dependence on diameter may be an artifact due to the limited number of thick fibers that can be injected in a sample of fixed mass.

Although the published injection studies indicate that potency decreases with decreasing length, researchers in these earlier studies were reluctant to identify a length below which contributions to carcinogenicity can be considered inconsequential. This may be due in part to the skewed distribution of fiber sizes typical of asbestos dusts. Thus, for example, even if structures less than 5 μm are only 1% as potent as structures longer than 5 μm, they may be as much as 100 times as plentiful in some asbestos dusts, so that the total contribution to potency would be equal for both size fractions.

Reasonable dose-response curves have been generated using various sample masses of a single material in some of these studies. This has been demonstrated for UICC crocidolite and UICC chrysotile "A" (Bolton 1984). Results indicate that the relationship between tumor incidence and the log of the dose may be linear and there is no effective threshold. A consistent difference between the two dusts is apparent; the points lie along separate curves and chrysotile appears to be more potent per unit sample mass.

In general, the analytical techniques used for quantifying size distributions in these studies are not fully documented. To the extent that they are, it appears that similar approaches were adopted to those described for the implantation studies above. Consequently, similar limitations apply to the interpretation of results. Briefly, large uncertainties are likely associated with counts of long fibers and estimates of the number of fibers per unit sample mass. Counts in several of the studies also suffer from limitations in the ability of SEM or PCM to detect thin fibers (Section 4.3); whenever SEM or PCM was employed, the thinner fibers were likely under-represented in reported fiber size distributions.

Because samples are placed against mesenchyme in the published implantation and injection studies, results of these studies most directly represent processes associated with the induction of mesothelioma. Assuming, however, that clearance and degradation processes are similar in the deep lung, once a fiber reaches a target tissue, results from the implantation and injection studies may also provide a model of biological response in lung tissue and the factors that lead to the induction of pulmonary tumors. Such a model must be considered qualitative at best, however, because it has been shown that the mechanisms of tissue response to the presence of asbestos in lung parenchyma and in the mesenchyme differ in detail (Section 6.3). The time periods over which the various clearance mechanisms operate in the deep lung and the mesenchyme also differ (Section 6.2), although, it is apparent that the general nature of the clearance and degradation processes in the two tissue types are generally similar.

6.4.2 Animal Inhalation Studies

Animal inhalation studies measure response to exposure in controlled systems that model most of the relevant variables associated with asbestos disease mechanisms in humans (including respirability, retention, degradation, clearance, translocation, and tissue-specific response). Thus, the available inhalation studies are the best database from which to evaluate the integrated effects that lead to the development of asbestos-related disease. Such studies can be used both to identify the characteristics of asbestos that determine biological activity and to qualitatively elucidate the nature of the corresponding relationship between exposure via inhalation and the induction of disease.

In this section, the existing animal inhalation studies are reviewed. In the following section, a project undertaken to overcome the limitations of the existing animal inhalation studies is described (the supplemental inhalation study). Because this latter project was specifically designed to support the risk protocol presented in this document, the nature and results of this project are described in detail.

The existing animal inhalation database consists of approximately 30 studies of which approximately 20 contain dose-response information based on lifetime monitoring of exposed animals, including the work by: Bellman et al. (1986, 1995); Bolton et al. (1982); Davis et al. (1978, 1980, 1985, 1986a,d, 1988a,b);

Goldstein et al. (1983); Le Bouffant et al. (1987); Lee et al. (1981); McConnell et al. (1982); Muhle et al. (1987); Platek et al. (1985); Smith et al. (1987); and Wagner et al. (1974, 1982, 1985, 1987). The studies are similar in overall design, although differences in experimental details potentially affect the comparability of results from separate studies.

In the inhalation studies, plugs formed from bulk samples of fibrous asbestos and related materials are placed in a dust generator and aerosolized. The generators (Beckett 1975), usually a modified version of the apparatus originally designed by Timbrell et al. (1968), consist of a rotating brush that sweeps over an advancing plug of bulk material and liberates fibers that are entrained in the controlled air flow passing through the device. The airborne dust is then passed either into a delivery system for nose-only exposure or into an exposure chamber where animals are kept for fixed periods of time (usually 7 hours per day) on a weekly routine (typically 5 days per week). The exposure routine is continued for as long as 2 years in some of the studies. In some, but not all of the studies, fiber-containing air is passed through a cyclone or elutriator prior to the exposure chamber so that exposure consists primarily of particle sizes within the respirable range.

Asbestos concentrations in the animal inhalation experiments are monitored by a combination of techniques. The concentration of total dust in the chamber is generally monitored gravimetrically. Simultaneously, membrane filter samples are collected and fibers counted by PCM. The quotient of these two measurements yields the number of (PCM) fibers per unit mass of dust (Section 4.3). The distribution of fiber sizes within the dusts introduced into the animal exposure chambers may also be determined in these studies by any of a variety of methods. As indicated previously (Section 4.3), however, the utility of such measurements depends on the precise manner in which they are derived.

To derive fiber size distributions, dust samples from these studies have generally been collected on polycarbonate filters for analysis by SEM. However, such distributions suffer both from the limitations of SEM (Section 4.3) and from the manner in which they are tied to the inhalation experiments (see Chapter 5).

Theoretically, the dose of any fiber size fraction can be estimated in a two-step process. The procedure incorporates consideration of a size fraction termed the PCM-equivalent fraction (PCME), which is the fraction of structures measured by SEM (or TEM) that correspond to the size range of structures known to be visible and therefore countable by PCM. First, the concentration of the PCM-equivalent fraction of the fiber size distribution (measured by SEM) is normalized by dividing its value by the PCM-measured concentration per unit dust mass observed in the inhalation experiment. This ratio is then multiplied by the fractional concentration of any specified size range of interest within the distribution (measured by SEM) to determine the exposure level for that size fraction. However, because bivariate (length by diameter) size distributions have not typically been developed in the available studies and because the number of total fibers longer than 5 μm observed by SEM (without adjustment for width) does not correspond to the number of total fibers longer than 5 μm observed by PCM, it is not possible to derive a true PCME fraction from the SEM data. Therefore, the theoretical approach described above for estimating exposure to specific size fractions cannot generally be applied in the existing studies.

Note that SEM analyses are typically conducted on limited dust samples only to provide information on size distributions. SEM is not used routinely to monitor daily asbestos concentrations in these experiments. Therefore a procedure like that described above is required to link the absolute concentrations to which rats are exposed to the measured and relative size distributions that are determined by SEM.

As indicated above, the data within the published animal inhalation studies are further constrained by the limitations of the analytical methods employed to generate the data (Section 4.3). Comparison of data between studies is also hindered by the lack of sufficient documentation to indicate the specific methods

and procedures employed in each study. Frequently, for example, it is unclear whether respirable dusts or total dusts have been monitored. Also, several studies fail to report one or both of two critical pieces of information: fiber-number-to-mass conversion factors and fiber size distributions. In addition, few studies indicate the precise counting rules employed for generating size distributions.

When structure-number-to-mass conversion factors are provided, unless the conversion factor is derived by counting fibers in a specific size range in a known mass of sample, and fiber concentrations in other size ranges are normalized to this count, several types of error may be introduced. For example, if total sample mass is assumed proportional to calculated mass derived from volume characterizations of the particles counted, unless isometric particles are sized along with fibers and both asbestos and nonasbestos particles are included in the count, a bias will be introduced in the conversion factor because total sample mass will have been under-represented to the extent that such particles are ignored in the estimation of fiber mass. Even if such particles are included, significant uncertainty may result from estimating the volumes of irregular particles and the limited precision associated with the count of the largest particles (due to their limited number). The uncertainty in the measurement of a fiber's diameter is squared in contributing to the uncertainty associated with a mass estimate.

Among reported variations in study design, differences in the detailed design and operation of the aerosolization chamber and the frequency and duration of exposure also potentially contribute to variation in results between studies. Also, use of differing animal strains and species across the various studies suggest the possibility that physiological differences may contribute to the observed variation in study results. Such differences are discussed further in Chapter 5.

A small subset of the asbestos dusts evaluated in the animal inhalation studies have been analyzed by TEM. However, even the published fiber size distributions from these TEM studies are subject to variation from differences in procedures used for sample preparation, from differences in counting rules, and from precision limitations due to the limited number of fibers actually characterized (Section 4.3). This latter limitation particularly affects the precision with which longer fibers are counted.

Although fiber-size distributions are primarily based on SEM analyses rather than TEM analyses in the existing animal inhalation studies, results generally echo the results of the injection and implantation studies. Thus, longer fibrous structures are observed to contribute most to asbestos biological activity, at least qualitatively. For example, dusts containing predominantly long amosite or long chrysotile fibers induce far more pulmonary tumors than samples containing predominantly short structures (Davis et al. 1986a,b). However, dusts evaluated in the existing inhalation experiments have not been characterized sufficiently to distinguish the dependence of biological activity on fiber diameter. Neither are the existing studies sufficient to evaluate the importance of mineralogy (or other potentially important asbestos characteristics) in determining risk.

6.4.3 Supplemental Inhalation Study

Given the problems with the existing animal inhalation studies, a project was undertaken to overcome some of the attendant limitations (Berman et al. 1995). To control for effects from variation in study design and execution (including choice of animal strain, animal handling procedures, equipment design, sample handling procedures, dosing regimen, and pathology protocols), the project focused on a set of studies generated from a single laboratory (i.e., the studies published by Davis and coworkers). Ultimately, the results from six studies covering nine different asbestos samples (including four types of asbestos with samples exhibiting multiple size distributions for two asbestos types) and a total of 13 separate experiments (some samples were studied at multiple exposure levels or in duplicate runs) were pooled for analysis. The database of experiments employed in the project is described in Table 6-7.

To overcome the limitations in the Davis et al. studies associated with the characterization of asbestos itself, the dusts studied in the thirteen experiments listed in Table 6-7 were regenerated by the same group who performed the original studies, from the same starting materials, using the same equipment, and reproducing the same conditions under which the original studies were conducted. Samples of the regenerated dusts were then collected and analyzed by TEM using a modified version of the Superfund air method (Chatfield and Berman 1990) to generate bi-variate size distributions that also include detailed characterization of the shapes and complexity of fibrous structures observed.

The total mass concentration of the regenerated dusts and fiber measurements by PCM were also collected to provide the data required to link size distributions in the regenerated dusts to absolute structure concentrations in the original inhalation experiments. The manner in which such calculations are performed has been published (Berman et al. 1995).

The concentration estimates (for asbestos structures exhibiting a range of characteristics of interest) that were derived from the TEM analyses of the regenerated dusts were then combined with the tumor response data from the set of inhalation experiments listed in Table 6-7 and a statistical analysis was completed to determine if a measure of asbestos exposure could be identified that satisfactorily predicts the lung tumor incidence observed. A more limited analysis was also performed to address mesothelioma; the small number of mesotheliomas observed Davis et al. studies constrained the types of analyses that could be completed for this disease. The detailed procedures employed in this analysis and the results from the first part of the study have been published (Berman et al. 1995). These are summarized below along with results from the parts of the study that remain to be published.

Table 6-7. Summary Data for Animal Inhalation Experiments Conducted by Davis and Coworkers[a,b]

Fiber Type	Description	Abbreviations	Mass Concentration (mg/m^3)	PCM f/ml	Number of Animals	Number of Benign Pulmonary Tumors	Number of Malignant Pulmonary Tumors	Total Number of Pulmonary Tumors	Meso-theli-omas	Reference
Chrysotile	UICC-A	UC	2	390	42	6	2	8	1	Davis et al. 1978
Chrysotile	UICC-A	UC	10	1,950	40	7	8	15	0	Davis et al. 1978
Chrysotile	Long	LC	10	5,510	40	8	12	20	3	Davis et al. 1988a
Chrysotile	Short	SC	10	1,170	40	1	6	7	1	Davis et al. 1988a
Chrysotile	UICC-A	UC	9.9	2,560	36	6	8	14	0	Davis et al. 1988b
Chrysotile	UICC-A (Discharged)[c]	DC	9.9	2,670	39	4	6	10	1	Davis et al. 1988b
Chrysotile	WDC Yarn[d]	WC	3.6	679	41	5	13	18	0	Davis et al. 1986b
Amosite	UICC	UA	10	550	43	2	0	2	0	Davis et al. 1978
Amosite	Long	LA	10	2,060	40	3	8	11	3	Davis et al. 1986a
Amosite	Short	SA	10	70	42	0	0	0	1	Davis et al. 1986a
Crocidolite	UICC	UR	4.9	430	43	2	0	2	1	Davis et al. 1978
Crocidolite	UICC	UR	10	860	40	1	0	1	0	Davis et al. 1978
Tremolite	Korean	KT	10	1,600	39	2	16	18	2	Davis et al. 1985
None	Control	C	0		20	0	0	0	0	Davis et al. 1978
None	Control	C	0		36	0	0	0	0	Davis et al. 1985
None	Control	C	0		61	1	1	2	0	Davis et al. 1986a
None	Control	C	0		64	1	1	2	0	Davis et al. 1986b
None	Control	C	0		47	1	1	2	0	Davis et al. 1988a

[a]Source: Berman et al. 1995

[b]Exposure occurred for 7 hours per day, 5 days per week for 1 year.

[c]UICC-A chrysotile in this experiment was treated with mixed polarity air (produced with a source of beta radiation) following generation to reduce the surface charge on individual particles within the dust.

[d]Chrysotile samples used for dust generation in this experiment were obtained from material treated by a commercial wet dispersion source.

In the statistical analysis performed in this study, the individual dose-response profiles from each of the two data sets were fit to a linear dose-response model:

$$P_i=1 - \exp(- Q_o - b_i \sum_j a_j x_{ij}) \qquad \text{(Eq. 6-7)}$$

where:

"P_i" is the probability of inducing pulmonary tumors observed in the "ith" study;

"Q_o" is a parameter that accounts for the background incidence of pulmonary tumors (assumed to be the same in all studies);

"x_{ij}" is the concentration of the "jth" size fraction of fibers in the "ith" study;

"a_j" is the coefficient of potency for the "jth" size fraction of fibers; and

"b_i" is a coefficient that represents the absolute potency of asbestos. In some analyses this coefficient is allowed to assume different values for different types of asbestos (e.g., chrysotile vs. amphibole), or other differences in experimental conditions.

The "a_j"s in this analysis are constrained to be positive because it is assumed that no fiber prevents cancer. The "a_j"s are also constrained to sum to 1.0, which means that they represent relative potency rather than absolute potency. Asbestos size fractions evaluated represent disjoint (mutually exclusive) sets.

The model (Equation 6-7) allows separate potency coefficients to be assigned to individual size fractions in a dose-response relationship that depends on multiple size fractions. Simultaneously, the "b" coefficients allows separate potencies to be assigned to different fiber types or to results from different studies performed under different experimental conditions.

Several investigators (Bertrand and Pezerat 1980; Bonneau et al. 1986; Stanton et al. 1977; Wylie et al. 1987) have used a logit curve to investigate the dose-response relating various measures of asbestos exposure to tumor response. The logit formula specifies that the tumor probabilities satisfy the relation:

$$\log[P/(1-P)]=a + b \cdot \log x \qquad \text{(Eq. 6-8)}$$

where log x is some measure of asbestos exposure, such as log of concentration of fibers in some size range. In some instances, the logit model was expanded by replacing $b \cdot \log x$ with a term representing a linear combination of exposure indices, so that multiple exposure indices could be explored simultaneously. The models were fit using standard linear regression based on normal theory.

An equivalent form for the logit model is:

$$P=e^{a}x^{b}/(1 + e^{a}x^{b}) \qquad \text{(Eq. 6-9)}$$

Written in this form, it is clear that this model does not permit a background response (i.e., P=0, whenever x=0). This is not a serious limitation when there are no tumors in control animals, such as was the case in Stanton et al. (1977). However, the model will not adequately fit data in which tumors are found in control animals. This was one reason for adopting the linear model (Equation 6-7) used in the investigation of the animal data reported in the study described here.

There is no evidence from this study that the linear model is inadequate. For cases in this study in which the fit between exposure and response is shown to be inadequate, the lack of fit is typically observed to be due to an inconsistent (non-monotonic) dose-response curve so that there is no indication that a non-linear model, such as the logit, would provide a better fit.

The linear model (Equation 6-7) used in this study was fit using a maximum likelihood (Cox and Lindley 1974) approach that utilizes the actual underlying binomial probabilities. This is a more efficient estimation method than use of regression methods based on normal theory, which was the fitting method used in the earlier studies (described above). In addition, the regression procedures applied in the earlier studies indicate only whether the exposure measures that were studied are significantly correlated with tumor response. In contrast, statistical goodness of fit tests were applied in this study to determine whether exposures that are described by a particular characteristic (or combination of characteristics) satisfactorily *predict* the observed tumor incidence. To illustrate, it is apparent from Text Figure 2 of Stanton et al. (1981) that the exposure measure they identify as being most highly correlated with tumor incidence (fibers longer than 8 μm and thinner than 0.25 μm) does not provide an acceptable fit to the observed tumor incidence. Similarly, although all of the univariate exposure measures listed in Table 2 of Berman et al. (1995) are highly correlated with tumor incidence, none of them adequately describe (fit) lung tumor incidence.

To test for goodness-of-fit in this study, each relationship was subjected to a chi-square goodness-of-fit test in which the fit of the model was rejected if the corresponding p-value was less than 0.05, indicating that the true model would provide a worse fit only 5% of the time. Among models that were not rejected based on a goodness-of-fit test, several hypotheses concerning the relative merit of the various models were also examined using the method of maximum likelihood (Cox and Lindley 1974).

An example of an adequate fit to the tumor response data is provided in Figure 6-5 (Figure 3 of Berman et al. 1995). Note that Figures 2 and 3 of the original paper were inadvertently switched during publication; the correct Figure 3 is reproduced here. The exposure index plotted in Figure 6-5 is the sum:

$$\text{Exposure}=a_1 x_{i1} + a_2 x_{i2} + a_3 x_{i3}=0.0017C_1 + 0.853C_2 + 0.145C_3 \qquad \text{(Eq. 6-10)}$$

Figure 6-5. Fit of Model. Tumor Incidence vs. Structure Concentration by TEM (Length Categories 5–40 μm, >40μm, Width Categories: <0.3 μm and >5 μm)

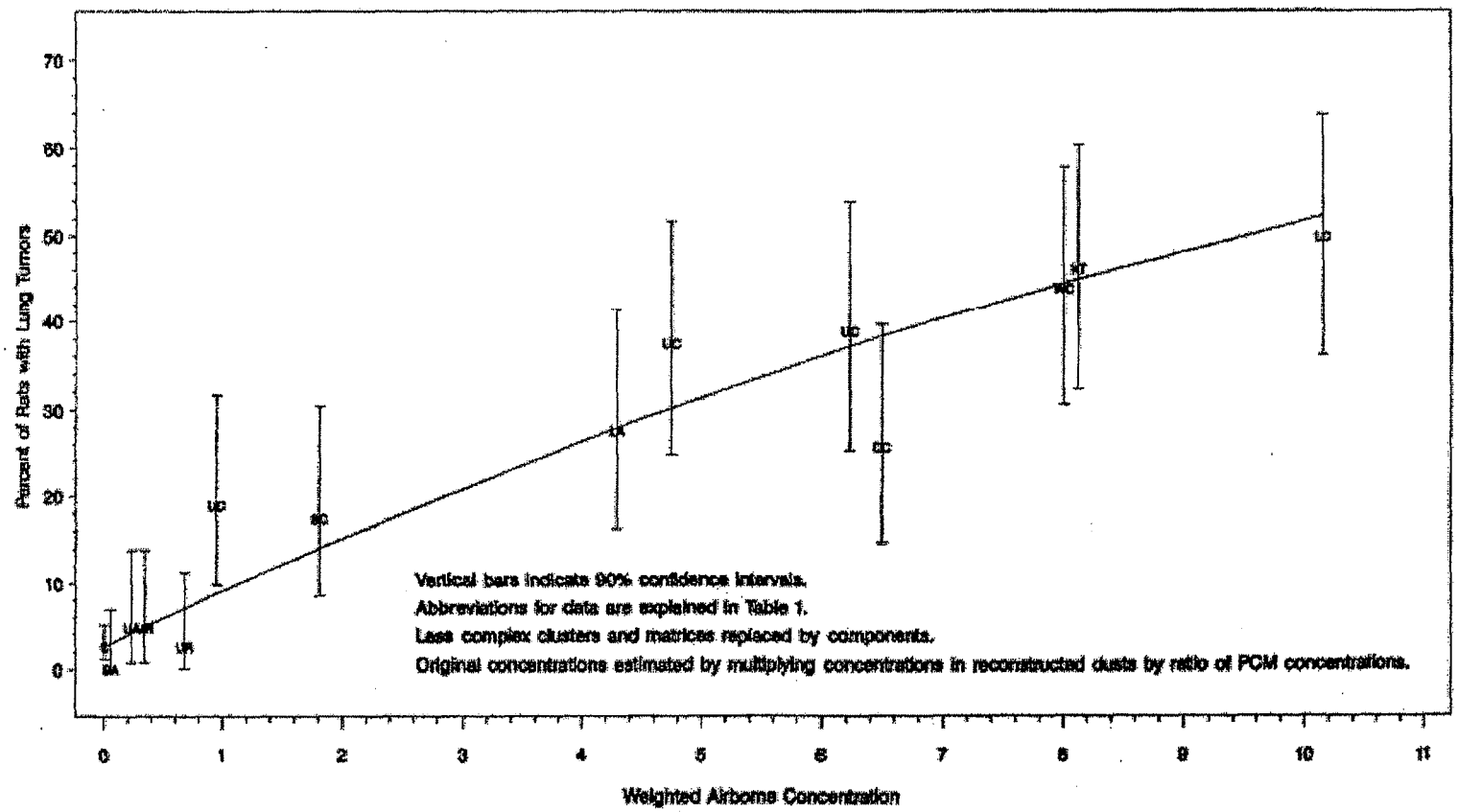

where:

"C_1" ($= x_{i1}$) is the concentration of structures between 5 and 40 μm in length that are thinner than 0.3 μm;

"C_2" ($= x_{i2}$) is the concentration of structures longer than 40 μm that are thinner than 0.3 μm; and

"C_3" ($= x_{i3}$) is the concentration of structures longer than 40 μm that are thicker than 5 μm.

This index of exposure represents one of the optimum indices reported in Berman et al. 1995.

As is clear from the figure, when exposure is expressed in the manner described above, the tumor responses observed in the 13 separate experiments that were evaluated increase monotonically with increasing exposure. It is also apparent that the data points representing each study fall reasonably close to the line representing the optimized model for this exposure index. This was verified by the fact that the corresponding goodness-of-fit test p-value was greater than 0.05. Thus, exposure adequately predicts response.

Results obtained from completing more than 200 statistical analyses to determine whether various measures of asbestos exposure adequately predict lung tumor response (Berman et al. 1995) indicate that:

- neither total dust mass nor fiber concentrations determined by PCM adequately predict lung tumor incidence;
- no univariate measure of exposure (i.e., exposure represented by the concentration of a single size category of structures as measured by TEM) was found to adequately predict lung tumor incidence. Of the univariate measures of exposure examined, the concentration of total structures longer than 20 μm provides the best fit (although still inadequate); and
- lung tumor incidence can be adequately predicted with measures of exposure representing a weighted sum of size categories in which longer structures are assigned greater potency than shorter structures.

The set of analyses completed in support of this work are summarized in Appendix C.

One example of an exposure measure that adequately describes lung tumor incidence is presented in Figure 6-5. Another exposure index shown to provide an adequate fit is:

$$0.0024C_a + 0.9976C_b \qquad \text{(Eq. 6-11)}$$

where:

"C_a" is the concentration of structures between 5 and 40 μm in length that are thinner than 0.4 μm; and

"C_b" is the concentration of structures longer than 40 μm that are thinner than 0.4 μm.

The fit of this index is depicted in Figure 6-6.

In addition to the above, a series of hypotheses tests were also conducted to test such questions as: whether fiber type affects potency or whether the component fibers in complex clusters and matrices should be counted individually. Questions concerning whether mesothelioma incidence can be adequately described by the same measure(s) of exposure that describe lung tumor incidence were also addressed. Taken as a whole, the results presented in Berman et al. (1995) support the following general conclusions:

- structures contributing to lung tumor incidence are thin (<0.5 μm) and long (>5 μm) with structures longer than 20 μm being the most potent;
- the best estimate is that short structures (<5 μm) are non-potent. There is no evidence from this study that these structures contribute anything to risk;
- among long structures, those shorter than 40 μm appear individually to contribute no more than a few percent of the potency of the structures longer than 40 μm;
- lung tumor incidence is best predicted by measurements in which the component fibers and bundles of complex structures are individually counted;
- at least for lung tumor induction in rats, the best estimate is that chrysotile and the amphiboles are equipotent;
- for equivalent size and shape structures, amphiboles are more potent toward the induction of mesothelioma than chrysotile; and
- after adjusting for the relative potencies of fiber type, the size categories that contribute to lung tumor incidence appear also to adequately describe mesothelioma incidence.

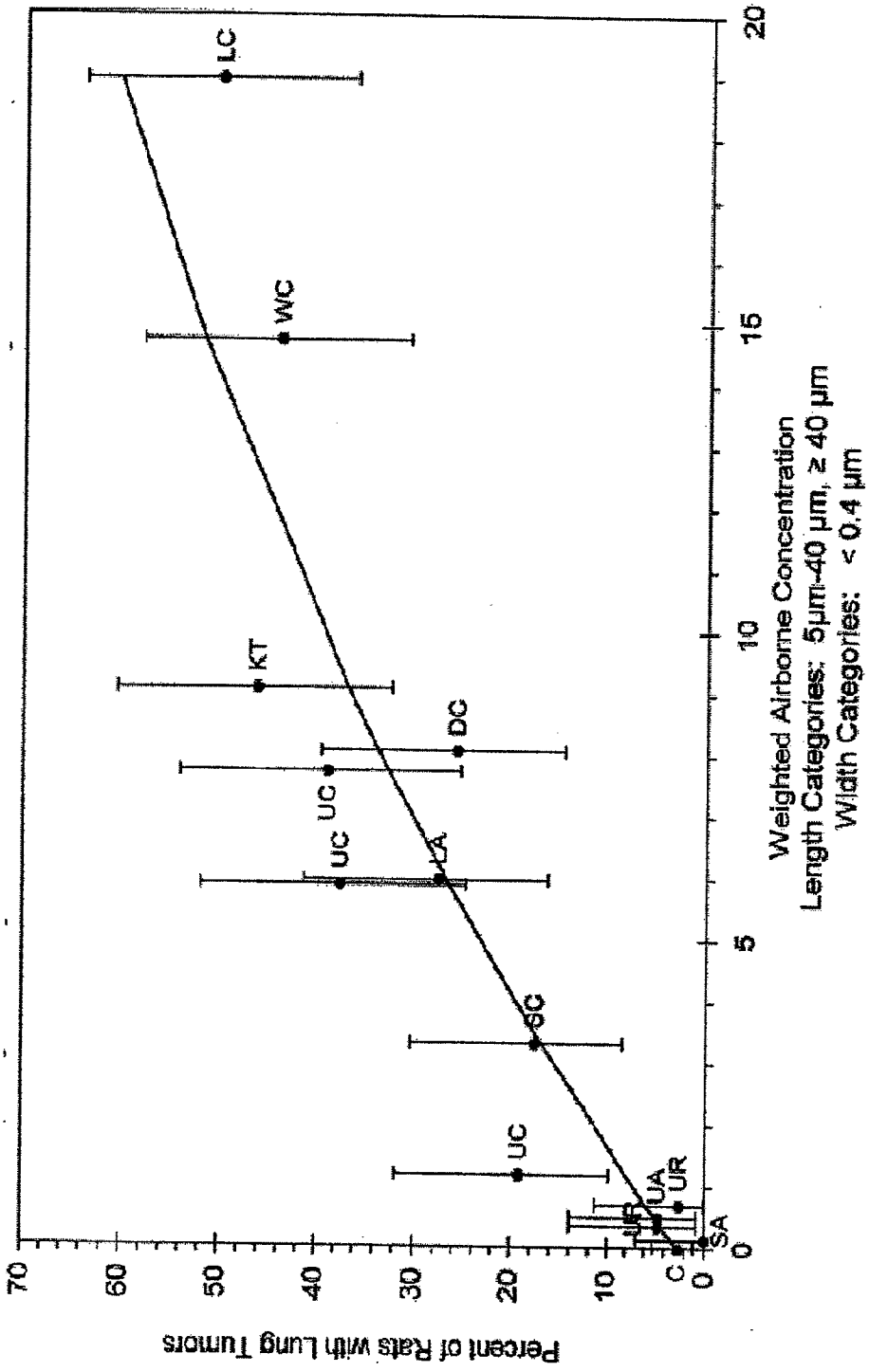

Figure 6-6. Fit of Model. Tumor Incidence vs. Structure Concentration by TEM (Length Categories 5–40 µm, >40µm, Width Categories: <0.4 µm)

A number of supplemental analyses were also conducted, primarily to identify optimal procedures for performing asbestos analysis and for estimating concentrations. These analyses have not yet been published, but they are included in the summaries in Appendix C. The most important results of the supplemental analyses are that:

- tumor incidence can only be adequately fit by data derived from TEM analysis of samples prepared by a direct transfer procedure. Measurements derived from indirectly prepared samples could not be fit to lung tumor incidence in any coherent fashion; and

- it was not possible to identify an exposure measure in which potency is expressed in terms of a single, continuous function of structure length.

Regarding the last point, although we were not able to identify a continuous function of length that provides an adequate fit to the tumor incidence data, the general results from the above analysis are not inconsistent with the hypothesis that potency is a continuous function of length (i.e., the Pott hypothesis, Pott 1982). The Pott hypothesis suggests that relative potency is low for short fibers, rises rapidly over an intermediate range of length, and approaches a constant for the longest fibers.

6.4.4 Conclusions Concerning Animal Dose-Response Studies

Results from our evaluation of the animal dose-response data for asbestos (including the existing injection/implantation studies, the existing inhalation studies, and our supplemental study) indicate that:

- short structures (less than somewhere between 5 and 10 μm in length) do not appear to contribute to cancer risk;

- beyond a fixed, minimum length, potency increases with increasing length, at least up to a length of 20 μm (and possibly up to a length of as much as 40 μm);

- the majority of structures that contribute to cancer risk are thin with diameters less than 0.5 μm and the most potent structures may be even thinner. In fact, it appears that the structures that are most potent are substantially thinner than the upper limit defined by respirability;

- identifiable components (fibers and bundles) of complex structures (clusters and matrices) that exhibit the requisite size range may contribute to overall cancer risk because such structures likely disaggregate in the lung. Therefore, such structures should be individually enumerated when analyzing to determine the concentration of asbestos;

- for asbestos analyses to adequately represent biological activity, samples need to be prepared by a direct-transfer procedure; and

- based on animal dose-response studies alone, fiber type (i.e., fiber mineralogy) appears to impart only a modest effect on cancer risk (at least among the various asbestos types).

Regarding the last of the above bullets, that only a modest effect of fiber mineralogy was observed in the available animal dose-response studies (when large effects are observed among human studies, Chapter 7), may be due at least in part to the limited lifetime of the rat relative to the biodurability of the asbestos fiber types evaluated in these studies, although it is also possible that different mechanisms drive the effects observed in the animal studies than those that dominate for asbestos-induced cancers in humans and that such mechanisms depend more strongly on mineralogy. Other explanations are also possible. Issues relating to both fiber mineralogy and fiber size are addressed further in Section 6.5 and Chapter 7.

6.5 CONCLUSIONS FROM AN EVALUATION OF SUPPORTING STUDIES

Although gaps in knowledge remain, a review of the literature addressing the health-related effects of asbestos (and related materials) provides a generally consistent picture of the relationship between asbestos exposure and the induction of lung cancer and mesothelioma. Therefore, the general characteristics of asbestos exposure that drive the induction of cancer can be inferred from the existing studies and can be applied to define appropriate procedures for evaluating asbestos-related risk. Furthermore, although it would be helpful to definitively identify the underlying biochemical triggers and associated mechanisms that drive asbestos-induced cancer, this is not an absolute prerequisite for the development of a technically sound protocol for assessing asbestos-related risk.

As previously indicated (Sections 6.3.8), the biochemical mechanisms that potentially contribute to the induction of asbestos-induced cancer are complex and varied. Moreover, different mechanisms appear to exhibit differing dose-response characteristics (i.e., the various mechanisms do not all show the same kind of dependence on fiber size or fiber type). Some mechanisms, for example, suggest that fiber length is important and that only structures that are sufficiently long induce a response. In contrast, other mechanisms suggest that fibers (and even non-fibrous particles) may all contribute to response and that the magnitude of the response is a function of the total surface area of the offending fibers (or particles). Among these mechanisms, additionally, some suggest that fiber type (i.e., mineralogy) is not an important determinant of potency while other mechanisms indicate that fiber type is an important determinant of potency.

The existing studies are not currently adequate to support definitive identification of the specific mechanisms that drive the induction of asbestos-related cancer (versus other mechanisms that may contribute only modestly or not at all). However, whatever mechanisms in fact contribute to the induction of disease, they must be consistent with the gross characteristics of exposure that are observed to predict response in the available whole-animal dose-response studies and human epidemiology studies. Therefore, the implications from these latter studies regarding the dependence of asbestos-induced cancers on fiber size and type are reviewed here in some detail. Further, in Chapter 8, they are used to support development of a protocol for evaluating asbestos-associated risks.

Fiber Length. Fibers less than a minimum length between 5 and 10 μm do not appear to contribute to risk. This is supported both by the results of our re-analysis of the animal inhalation studies conducted by Davis and coworkers (Section 6.4.3 and Berman et al. 1995), in which this hypothesis was tested formally, and by inferences from the broader literature. As long as fiber size is adequately characterized, the animal inhalation studies (Section 6.4.2) and injection/implantation (Section 6.4.1) studies consistently indicate lack of ability of short structures to contribute to the induction of cancer. Furthermore, animal retention studies (Section 6.2.1) and histopathology studies (Section 6.2.2) provide strong mechanistic evidence that explains the lack of potency for short structures; they are readily cleared from the respiratory tract. Even when sequestered in large numbers in macrophages within the lung, there is little indication that such structures induce the kinds of tissue damage and related mechanisms that appear to be closely associated with the induction of cancer.

Although there are mechanism studies that may suggest a role for short fibers in the induction of asbestos-related disease (see, for example, Goodglick and Kane 1990, Section 6.3.4.4), such studies do not track cancer as an endpoint. Therefore, the relationship between the toxic endpoint observed and the induction of cancer needs to be adequately addressed before it can be concluded definitively that short structures can contribute to cancer. Moreover, such a conclusion would be surprising given the substantial evidence that exists to the contrary.

Beyond the minimum length below which structures may be non-potent, potency appears to increase with increasing length, at least up to a length of 20 μm and potentially up to a length of 40 μm. The latter limit is suggested by our re-analysis of the Davis et al. studies (Section 6.4.3) in which it was also found that structures longer than 40 μm may be as much as 500 times as potent as those between 5 and 40 μm in length. The former limit is suggested by broader inferences from the literature that suggest the cutoff in the length of structures that are at least partially cleared by macrophages from the lung may lie close to 20 μm and that the efficiency of clearance likely decreases rapidly for structures between 10 and 20 μm in length (Section 6.2). Such inferences are further reinforced by measurements of the overall dimensions of macrophages in various mammals by Krombach et al. (1997), as reported in Section 4.4.

Importantly, the inferences that potency increases for structures longer than 10 μm (up to some limiting length) from these various studies are strongly reinforcing, even though the upper limits to the points at which potency stops increasing do not precisely correspond. Furthermore, that the longest structures are substantially more potent than shorter structures (and that the shortest structures are likely non-potent) dictates that asbestos analyses performed in support of risk assessment need to provide adequate sensitivity and precision for counts of the longest structures.

Fiber Diameter. Because fibers that contribute to the induction of cancer must be respirable, they must also be thin. The studies reviewed in Section 6.1 indicate that respirable fibers are thinner than 1.5 μm and the vast majority of such structures are thinner than 0.7 μm. In fact, the results of injection, implantation, and inhalation studies reviewed in Sections 6.4.1 and 6.4.2 and the results of our supplemental re-analysis of the Davis et al. studies (Section 6.4.3) indicate that the fibers that contribute most to the induction of asbestos-related cancers are substantially thinner than the limit suggested by respirability alone.

Importantly, the results of all of the studies cited above indicate that it is a cutoff in absolute width that defines the bounds of biological activity rather than a cutoff in aspect ratio (the ratio of length to width) that has been used to define fibrous structures heretofore. That is why the exposure index recommended based on our review of the studies by Davis and coworkers incorporates a maximum width as a cutoff, rather than a minimum aspect ratio.

Fiber Complexity. In our supplemental evaluation of the Davis et al. studies (Section 6.4.3), the tumor incidence data from the animal inhalation studies were best fit (predicted) by exposure indices in which the component fibers and bundles of complex structures (clusters and matrices) were separately enumerated and included in the exposure index used to represent concentration (Section 6.4.3). The appropriateness of such an approach is further supported by the observation that loosely bound structures (including, for example, chrysotile bundles) readily disaggregate *in vivo* (Section 6.2). Therefore, it is recommended in this report that those components of complex structures that individually exhibit the required dimensional criteria be individually enumerated and included as part of the count during analyses to determine the concentration of asbestos in support of risk assessment.

Fiber Type (Mineralogy). The magnitude of any effect of mineralogy upon cancer risk in rodents appears to be modest at best. On the other hand, mineralogy appears to be an important determinant for cancer risk in human epidemiology studies (Chapter 7), with chrysotile appearing less potent than amphibole for inducing mesothelioma and (with lesser certainty) lung cancer. This difference may be due to differences in the life spans of rats and humans compared to the differential biodurability of the different fiber types. It must also be emphasized that, due to confounding, the effects of fiber size and fiber mineralogy need to be addressed simultaneously, if one is interested in drawing useful conclusions concerning fiber mineralogy.

Results from some (but not all) of the animal injection, implantation, and inhalation studies previously reviewed (Sections 6.4.1 and 6.4.2) suggest that mineralogy plays an important role in determining biological activity. However, the nature of the effects of mineralogy are not easily separated from size effects, due to the methodological limitations of the studies cited. Therefore, the evidence from these studies can be considered ambiguous. Formal hypothesis testing during the re-analysis of rat inhalation studies (Section 6.4.3) indicates that, when size effects are addressed, chrysotile and the amphiboles exhibit comparable potency toward the induction of lung cancer. In contrast, amphiboles were estimated to be approximately 3 times more potent than chrysotile toward the induction of mesothelioma, once fiber size effects are addressed.

Several of the human pathology studies cited previously (Section 6.2.3) suggest that mineralogy is an important factor in determining cancer risk, but these studies similarly suffer from methodological difficulties that introduce ambiguity into the inferences drawn. However, it is clear from the human epidemiology data (Chapter 7) that mineralogy plays a substantial role in the determination of risk for human cancer (primarily, mesothelioma).

The underlying cause(s) for the observed difference in potency between chrysotile and the amphiboles may relate to differences in fiber durability (Section 6.2), to size/shape related differences in fibers that are a function of mineralogy and that cause differences in deposition, retention, or translocation (Sections 6.1 and 6.2), and/or to the dependence on mineralogy of the

specific mechanisms underlying the biological responses of specific tissues (Section 6.3). The relative magnitudes of such effects on animal and human pathology also need to be considered, if the observed differences in potency among animal and human studies, respectively, is to be reconciled. Such considerations are addressed further in Chapter 8.

Importantly, whether the observed differences in the role of mineralogy toward animal and human pathology can be reconciled, the effects of mineralogy can be adequately addressed when assessing asbestos-related cancer risk for humans by incorporating dose-response coefficients explicitly derived from the human epidemiology data. Because this is the approach proposed in this document, effects due to mineralogy are properly addressed.

An Appropriate Exposure Index for Risk Assessment. The optimum exposure index defined based on the re-analysis of the animal inhalation studies conducted by Davis and coworkers (Section 6.4.3) is a weighted sum of the concentrations of (1) structures between 5 and 40 μm in length that are thinner than 0.4 μm, and (2) structures longer than 40 μm that are thinner than 0.4 μm (Equation 6-11).

This index was shown to adequately fit (predict) the tumor incidence data across the 13 separate animal inhalation experiments evaluated (P=0.09). Whether the exposure index defined in Equation 6-11is also optimal for capturing the relevant characteristics of fibers that contribute to the induction of human cancer is an open question. Because it captures the major characteristics (concerning length and diameter) identified above that are indicated to be important for human exposures, it represents a promising candidate. Unfortunately, however, the data required to match this index to a set of human-derived exposure-response coefficients does not currently exist (Section 7.4). Therefore, compromises are required to apply the general conclusions of this Chapter to the human data. These are addressed further in Section 7.4.1.

7.0. EPIDEMIOLOGY STUDIES

The existing epidemiology studies provide the most appropriate data from which to determine the relationship between asbestos exposure and response in humans. As previously indicated, however, due to a variety of methodological limitations (Section 5.1), the ability to compare and contrast results across studies needs to be evaluated to determine the confidence with which risk may be predicted by extrapolating from the "reference" epidemiology studies to new environments where risk needs to be assessed. Reliable extrapolation requires both that the uncertainties contributed by such methodological limitations and that several ancillary issues (identified in Chapter 2) be adequately addressed.

A detailed discussion of the methodological limitations inherent to the available epidemiology studies was provided in the Health Effects Assessment Update (U.S. EPA 1986) and additional perspectives are provided in this document (Section 5.1). The manner in which the uncertainties associated with these limitations are addressed in this document are described in Appendix A. As previously indicated (Chapter 2), the ancillary issues that need to be addressed include:

(1) whether the models currently employed to assess asbestos-related risk adequately predict the time and exposure dependence of disease;

(2) whether different mineral types exhibit differential potency (and whether any differences in potency relate to the relative *in vivo* durability of different asbestos mineral types);

(3) whether the set of minerals included in the current definition for asbestos adequately covers the range of minerals that potentially contribute to asbestos-related diseases; and

(4) whether the analytical techniques and methods used to characterize exposures in the available epidemiology studies adequately capture the characteristics of exposure that affect biological activity.

All but the third of the above issues are addressed in this chapter. Currently, the third issue can best be addressed by evaluating inferences from the broader literature (see Chapter 6). The remaining issues are addressed separately for lung cancer and mesothelioma following a brief overview of the approach adopted for evaluating the epidemiology literature.

7.1 APPROACH FOR EVALUATING THE EPIDEMIOLOGY LITERATURE

To develop exposure-response relationships (and corresponding exposure-response coefficients) for use in risk assessment from epidemiological data, two basic types of information are necessary: information on the disease mortality experienced by each member of the study population (cohort) and information on the asbestos exposure experienced by each member of the cohort. So that disease mortality attributable to asbestos can be distinguished from other (background) causes of death, it is also necessary to have knowledge of the rates of mortality

that would be expected in the study population, absent exposure. Normally, such information must be determined based on a "reference" or "control" population.

Ideally, one would like to have complete knowledge of exposure at any period of time for each individual in the cohort and complete access to the data to fit different types of exposure/response models to the data so that the approach for evaluating the relationship between exposure and response can be optimized. In most instances, unfortunately, the data suffer from multiple limitations (see Section 5.1 and Appendix A) and the analysis is further constrained by less than complete access to the data.

Briefly, the major kinds of limitations that potentially contribute to uncertainty in the available epidemiology studies (and the effect such limitations likely produce in estimates of exposure-response coefficients) include:

- limitations in the manner that exposure concentrations were estimated (contributing to variation across studies);
- limitations in the manner that the character of exposure (i.e., the mineralogical types of fibers and the range and distribution of fiber dimensions) was delineated (contributing to systematic variation between industry types and, potentially, between fiber types);
- limitations in the accuracy of mortality determinations or incompleteness in the extent of tracing of cohort members (contributing to variation across studies);
- limitations in the adequacy of the match between cohort subjects and the selected control population (contributing to variation across studies and may have a substantial effect on particular studies); and
- inadequate characterization of confounding factors, such as smoking histories for individual workers (contributing to variation across studies and may have a substantial effect on particular studies).

More detailed discussion of the above limitations is provided in Section 5.1. The manner in which these limitations are being addressed in this evaluation are described briefly below and in more detail in Appendix A.

The existing asbestos epidemiology database consists of approximately 150 studies of which approximately 35 contain exposure data sufficient to derive quantitative exposure/response relationships. A detailed evaluation of 20 of the most recent of these studies, which includes the most recent follow-up for all of the cohorts evaluated in the 35 studies, based on the considerations presented in this overview, is provided in Appendix A.

This new analysis of the epidemiology database differs from the evaluation conducted in the 1986 Health Effects Assessment Update (U.S. EPA 1986) in several ways. It incorporates new studies not available in the 1986 update that contain information on exposure settings not previously evaluated as well as more recently available follow-up for exposure settings

previously evaluated. It also incorporates new features in the manner in which the analysis was conducted. These new features include:

- estimation of "uncertainty" bounds for the exposure-response coefficients (potency factors) derived from each study; and
- for the lung cancer model, introducing a parameter, α, which accounts for the possibility that the background lung cancer mortality rate in the asbestos-exposed cohort differs systematically from the rate in the control population.

The uncertainty bounds were developed to account for uncertainty contributed by the manner that exposure was estimated, by the manner that work histories were assigned, by limitations imposed by the manner in which results were reported in published papers, and by limitations in the accuracy of follow-up, in addition to accounting for the statistical uncertainty associated with the observed incidence of disease mortality. A detailed description of how the uncertainty bounds were constructed is provided in Appendix A.

Exposure-response coefficients were estimated for each cohort both by requiring that α=1 (the approach followed in the 1986 Health Effects Assessment Update, U.S. EPA 1986) and by allowing α to vary while fitting the lung cancer model to data. Allowing α to vary addresses potential problems due to differences in background lung cancer rates between the cohort and the control population due, for example, to differences in smoking habits in the two populations. As indicated in Appendix A, this adjustment has a substantial effect on the fit of the U.S. EPA model to the data for several specific cohorts and a corresponding effect on the estimates of the lung cancer exposure-response coefficients for those cohorts.

We were also able to obtain the original, raw data for selected cohorts from a limited number of the more important of the published epidemiology studies. This allowed us to more formally evaluate the appropriateness of the existing U.S. EPA models for lung cancer and mesothelioma (Sections 7.2 and 7.3).

Exposure-response coefficients, and corresponding risk estimates derived therefrom, must be based upon an "exposure index" that expresses the relative potency of asbestos fibers of different dimensions. For example, the exposure index utilized in the 1986 Health Effects Assessment Update (U.S. EPA 1986) assigns equal potency to all fibers longer than 5 μm that exhibit an aspect ratio >3 and a thickness >0.25 μm, regardless of type of asbestos, and assigns zero potency to shorter, squatter, or thinner fibers. In this update, we evaluated a range of such exposure indices, both with respect to agreement with evidence from the literature on the relative potency of asbestos structures of differing types and dimensions (Section 7.4) and with respect to overall agreement across the exposure-response coefficients derived from the available epidemiology studies and adjusted for exposure index. This analysis led to proposed new exposure indices that better reflect the evidence from the literature on the relative potency of different structures and provide improved agreement among exposure-response coefficients estimated from different environments. Such improvement in agreement across studies correspondingly increases the confidence with which the exposure-response factors derived from the existing studies can be applied to new environments.

7.2 LUNG CANCER

The 1986 U.S. EPA lung cancer model (U.S. EPA 1986) assumes that the relative risk, (RR), of mortality from lung cancer at any given age is a linear function of cumulative asbestos exposure in units of fiber-years/ml (f-y/ml) as measured by PCM, disregarding any exposure in the most recent ten years. This exposure variable is denoted by CE_{10}, and its use embodies the assumption that asbestos exposures during the most recent 10 years do not affect current lung cancer mortality risk. The mathematical expression for this model is:

$$RR = 1 + K_L * CE_{10} \qquad \text{(Eq. 7-1)}$$

where the linear slope, K_L, is termed the "lung cancer exposure-response coefficient." This parameter is generally estimated by fitting the model to data from an occupational mortality cohort study consisting of observed and expected numbers of cancer deaths categorized by cumulative exposure, with the expected numbers determined from age- and calendar-year-specific lung cancer mortality rates from an appropriate control population (e.g., U.S. males). This model predicts that the mortality rate in an asbestos-exposed population is the product of the mortality rate in an unexposed, but otherwise comparable, population, and the RR. Consequently the excess mortality due to asbestos is the product of the background mortality rate and the excess RR, $K_L * CE_{10}$. Since smokers have a higher background mortality from lung cancer, the model predicts a higher excess asbestos-related lung cancer mortality in smokers than in non-smokers.

To account for the possibility that an occupational cohort may have a different background mortality rate of lung cancer than the control population (e.g., due to different smoking habits or exposures to other lung carcinogens), in the present analysis Equation 7-1 is expanded to the form,

$$RR = \alpha * (1 + K_L * CE_{10}) \qquad \text{(Eq. 7-2)}$$

where α is the RR in the absence of asbestos exposure relative to the control population. This form of the model contains two parameters, the background RR, α, and the lung cancer exposure-response coefficient, K_L.

7.2.1 The Adequacy of the Current U.S. EPA Model for Lung Cancer

Access to the raw epidemiology data from two key studies allowed us to evaluate the adequacy of the U.S. EPA model (Equation 7-2) for describing the time and exposure dependence for lung cancer in asbestos-exposed cohorts. For this analysis, the raw data for the cohort of crocidolite miners in Wittenoom, Australia was graciously provided by Dr. Nick de Klerk (de Klerk 2001) and the raw data for the cohort of chrysotile textile workers (described by Dement et al. 1994) was graciously provided by Terri Schnoor of NIOSH (Schnoor 2001). The Wittenoom cohort was originally described by Armstrong et al. (1988), but the data provided by de Klerk includes additional follow-up through 1999.

7.2.1.1 Exposure Dependence

To evaluate the adequacy of the linear exposure response relationship assumed by the U.S. EPA lung cancer model, the lung cancer model (Equation 7-2) was fit to the raw data from both the South Carolina and Wittenoom cohorts. In these analyses, each person-year of follow-up was categorized by cumulative exposure defined using a lag of 10 years. The data were then grouped into a set of cumulative exposure categories and the observed and expected numbers of lung cancers were computed for each category. For South Carolina, expected numbers were based on sex-race-age- and calendar-year-specific U.S. rates. Separate analyses were conducted for white males, black males, and white females, as well as for the combined group. For Wittenoom expected rates were based on age- and calendar-year-specific rates for Australian men. The categorized data and the resulting fit of the model to the data from Wittenoom and South Carolina are presented in Tables 7-1 and 7-2, respectively.[1]

For the Wittenoom data (Table 7-1), the fit with α=1 is poor ($p<0.0001$), as the model overpredicts the number of cancers in the highest exposure category and underpredicts at lower exposures. By contrast the fit of the model with α variable is adequate ($p=0.1$). This model predicts a relatively high background of lung cancer in this cohort relative to Australian men in general (α=2.1) and a correspondingly shallow slope, with the RR increasing only from 2.1 at background to 3.6 in the highest exposure category. A test of the hypothesis that α=1 for this cohort is rejected ($p<0.01$) and the model fit to the data (with α variable) predicts K_L=0.0047 $(f/ml\text{-}yr)^{-1}$.

The fit of the U.S. EPA model to the South Carolina lung cancer data categorized by cumulative exposure is shown in Table 7-2. The model with α=1 cannot be rejected both when the model is applied to white males only ($p=0.54$) or with all data combined ($p=0.92$). Since the values α and K_L estimated from white males only are similar to those estimated using the complete cohort (black and white males and white females), the fit to the complete data is emphasized in this analysis. This fit predicts α=1.2 and K_L=0.021 $(f\text{-}y/ml)^{-1}$. A test of the hypothesis that α=1 for this cohort cannot be rejected ($p=0.21$), and in this fit K_L=0.028 $(f\text{-}y/ml)^{-1}$

[1]The fitting of the lung cancer model to the cohort data was carried out by assuming that the observed numbers of cancers in different exposure categories were independent, with each having a Poisson distribution with expectation equal to the expected number based on the control population times the relative risk predicted by Equation 7-2. In the computation of the relative risk for a cumulative exposure category, the person-year-weighted average cumulative exposure (lagged 10 years) for the category was used to represent the exposure in that category. With these assumptions, α and K_L were estimated by the method of maximum likelihood, confidence intervals were constructed using the profile likelihood method, and likelihood ratio tests were used to test hypotheses (Cox and Oakes 1984; Venson and Moolgavkar 1988).

Table 7-1. Fit of EPA Lung Cancer Model to Observed Lung Cancer Mortality Among Wittenoom, Australia Miners (Deklerk 2001) Categorized by Cumulative Exposure Lagged 10 Years

Cumulative Exposure Lagged 10 Years (f-y/ml)		Observed Deaths	Expected Deaths	Predicted Deaths by Model	
Range	Average			(α=1)	(α=2.1)
0	0	5	4.6	4.6	9.8
0–0.4	0.19	27	7.9	8.0	17.0
0.4–1.0	0.69	11	8.2	8.3	17.6
1.0–2.3	1.6	22	11.6	12.1	24.9
2.3–4.5	3.3	28	12.9	14.0	27.9
4.5–8.5	6.2	38	14.3	16.7	31.4
8.5–16	11.8	31	13.2	17.4	29.8
16–28	21.5	21	9.2	14.5	21.6
28–60	41.1	25	11.6	24.5	29.6
60+	142.0	43	11.6	56.5	41.6
Total		251	105.1	176.6	251.0
		Goodness of Fit P-value		<0.0001	0.1

Test of H_0: α=1
p<0.01

Estimates of K_L $(f\text{-}y/ml)^{-1}$

(α=1)
K_L=0.027
90% CI: (0.020, 0.035)

(α=2.1 [MLE])
K_L=0.0047
90% CI: (0.0017, 0.0087)

Table 7-2. Fit of EPA Lung Cancer Model to Observed Lung Cancer Mortality Among South Carolina Textile Workers (Schnoor 2001) Categorized by Cumulative Exposure Lagged 10 Years

Cumulative Exposure Lagged 10 Years (f-y/ml)		Observed Deaths	Expected Deaths	Predicted Deaths by Model	
Range	Average			(α=1)	(α=1.2)
0	0	0	0.9	0.9	1.1
0–0.5	0.35	4	2.6	2.7	3.2
0.5–1.0	0.75	7	5.5	5.6	6.8
1.0–2.5	1.7	10	9.7	10.1	12.1
2.5–4.5	3.4	13	7.9	8.6	10.2
4.5–8.5	6.2	11	7.7	9.1	10.5
8.5–16	11.8	11	7.2	9.6	10.9
16–28	21.3	8	5.3	8.4	9.2
28–60	41.5	14	6.3	13.8	14.3
60–80	69.2	9	3.0	9.0	9.0
80–110	93.3	10	2.9	10.8	10.5
110+	173	25	4.3	25.6	24.2
Total		122	63.4	114.1	122.0
		Goodness of Fit P-value		0.92	0.96

Test of H_0: α=1
p=0.21

Estimates of K_L $(f\text{-}y/ml)^{-1}$

(α=1)
K_L=0.028
90% CI: (0.021, 0.037)

(α=1.2 [MLE])
K_L=0.021
90% CI: (0.012, 0.034)

Appendix A contains fits of the model to published exposure-response data from 18 studies (all, with the exception of Wittenoom and South Carolina, obtained from the published literature). In each of these 18 cases the linear model (Equation 7-2) provides an adequate description of the exposure-response. However, α was estimated as >1.0 in 15 of these cases and statistically significantly so in six cases, compared to only one case where α was found to be significantly <1.0. If the true background lung cancer rates in these 15 cohorts with α>1.0 are equal to that in the corresponding control population (i.e., so that a fit with α=1.0 is appropriate), the exposure-response would appear to be supra-linear. At the same time, the data in 11 of the 18 studies (more than half) can be adequately fit with α=1.0 and the studies for which α=1.0 does not provide an adequate fit do not appear to be related by mineral type, by industry, or by the size of the study (Appendix A). Thus, while we completed our analysis using the current lung cancer

model (Equation 7-2), further evaluation of the lung cancer exposure-response relationship appears to be warranted.

7.2.1.2 Time Dependence

The lung cancer model (Equation 7-2) was next evaluated to determine whether it adequately describes the time-dependence of the lung cancer mortality observed in the Wittenoom and South Carolina cohorts. Of particular interest is whether the model accurately predicts lung cancer mortality many years after exposure has ceased. The model predicts that RR increases linearly with cumulative exposure lagged 10 years until 10 years following the end of exposure, after which it remains constant from that time forward. However, it has been suggested (e.g., Walker 1984) that RRs for lung cancer eventually decline after cessation of exposure. Any investigation of this issue should control for exposure level, since exposures can also fall with increasing time due to higher death rates in more heavily exposed subjects. The availability of the raw data from the South Carolina and Wittenoom cohorts provides an opportunity to explore this issue in more depth.

To investigate the assumption inherent in the lung cancer model (Equation 7-2) that the RR remains constant following the secession of exposure, bivariate tables were constructed from both the Wittenoom and South Carolina data in which observed and expected numbers of lung cancers were cross-classified by both cumulative exposure (using the same exposure categories as in Tables 7-1 and 7-2) and time since last exposure categorized using 5-year intervals. The lung cancer model (Equation 7-2) was then fit to these bivariate data. A formal statistical test was conducted of whether the lung cancer RR changed following the end of exposure. This test consisted of appending the multiplicative factor, exp(-K•TSLE), to the lung cancer model (Equation 7-2), where TSLE is time since last exposure, and conducting a likelihood ratio test of whether the estimated parameter, K, is statistically significantly different from zero. For presentation the bivariate tables were collapsed into univariate tables (Tables 7-3 and 7-4) categorized only by time since last exposure, by summing observed and expected cancers over cumulative exposure categories and computing person-year-weighted averages of cumulative exposure and times since last exposure.

Table 7-3 shows the resulting fit of the U.S. EPA lung cancer model to the Wittenoom lung cancer data categorized by time since last exposure. The RRs rise to a maximum between 10 and 30 years from last exposure and then decline thereafter. However, a very similar pattern is seen with cumulative exposure, which peaks between 10 and 15 years from last exposure, and then declines due to higher mortality among more heavily exposed workers. The U.S. EPA lung cancer model (which does not assume a decrease in RR with time, but does account for any decrease in exposure with increasing time since last exposure) provides an adequate fit to these data ($p=0.13$, α estimated), and there is no apparent tendency for the predicted deaths to fall below observed at the longest times since last exposure. To the contrary, the model-predicted number of lung cancer deaths more than 35 years since last exposure (53.3) is very close to, but slightly larger than, the observed number (51). Likewise, the parameter K was not significantly different from zero ($p=0.16$). Thus, the lung cancer model (Equation 7-2) provides a good description of the Wittenoom lung cancer data categorized by time since last exposure and there is no indication of a drop in the RR up to 45 or more years after exposure has ended that cannot be accounted for by reduced exposures in the longest time categories. It should also be noted

that the values of α (2.1) and K_L (0.0051 f/ml-y) estimated from this bivariate analysis are very similar to those estimated from the univariate analysis summarized in Table 7-1.

Table 7-3. Fit of EPA Lung Cancer Model to Observed Lung Cancer Mortality Among Wittenoom, Australia Miners (Deklerk 2001) Categorized by Years Since Last Exposure

Years Since Last Exposure		Average Exposure Lagged 10 Years (f-y/ml)	Observed Deaths	Expected Deaths	Relative Risk	Predicted Deaths by Model (α=2.1)
Range	Average					
0–1	0.27	1.2	0	0.6	0	1.5
1–5	3.0	1.2	1	1.6	0.6	3.9
5–10	7.5	7.7	8	3.9	2.0	10.3
10–15	12.5	24.8	19	7.0	2.7	19.2
15–20	17.5	24.1	26	11.4	2.3	29.1
20–25	22.5	22.8	42	16.4	2.6	39.8
25–30	27.4	22.0	54	20.1	2.7	47.2
30–35	32.3	21.7	50	20.3	2.5	46.6
35–40	37.1	20.0	31	13.9	2.2	31.4
40–45	43.3	16.7	20	9.6	2.1	21.1
45+	51.2	13.0	0	0.4	0	0.8
Total			251	105.1		250.9
			Goodness of Fit P-value			0.19

Table 7-4 shows the corresponding fit of the U.S. EPA lung cancer model to the South Carolina lung cancer data. This table indicates a marked decrease in RR with increasing time since last exposure. However, there is a concomitant decrease in cumulative exposure. The U.S. EPA lung cancer model provides an adequate fit to these data (p=0.31, α estimated), and the estimates of α (1.3) and K_L (0.20 $(\text{f-y/ml})^{-1}$) are very similar to those obtained from the univariate analysis (Table 7-2). There is no obvious tendency for the model to underestimate risk at the longest times since last exposure, and the value of K estimated for this cohort is not significantly different from zero (p=0.12).

Table 7-4. Fit of EPA Lung Cancer Model to Observed Lung Cancer Mortality Among South Carolina Textile Workers (Schnoor 2001) Categorized by Years Since Last Exposure

Years Since Last Exposure		Average Exposure Lagged 10 Years (f-y/ml)	Observed Deaths	Expected Deaths	Relative Risk	Predicted Deaths by Model (α=1.3)
Range	Average					
0–1	0.06	21.8	15	4.1	3.7	13.4
1–5	3.0	13.1	7	2.2	3.2	7.3
5–10	7.5	16.5	14	3.5	3.9	11.5
10–15	12.5	16.5	8	3.8	2.1	10.4
15–20	17.5	11.5	3	3.6	0.8	7.0
20–25	22.5	9.9	15	5.1	2.9	8.8
25–30	27.5	9.2	13	7.1	1.8	11.7
30–35	32.5	8.5	11	9.5	1.2	15.0
35–40	37.4	7.8	17	10.5	1.6	16.2
40–45	43.5	7.1	19	13.8	1.4	20.8
45+	50.4	31.6	0	0.0	0.0	0.0
Total			122	63.4		122.0
			Goodness of Fit P-value			0.31

Raw lung cancer data were not available from any additional studies, so that the corresponding analysis could not be performed on any other cohort. However, the report by Seidman et al. (1986) on workers at a factory in Patterson, New Jersey that utilized amosite as a raw material contains data in a form that permit a similar analysis using time since onset of exposure rather than time since last exposure. The result of this analysis is shown in Table 7-5, which corresponds to Tables 7-3 and 7-4 except that Table 7-5 presents mortality by time since first exposure rather than time since last exposure.[2] Since exposures in the Seidman study averaged

[2]Table 7-5 was created in the following manner. Table XIV of Seidman et al. (1986) contains expected numbers of deaths from all causes cross-classified by cumulative exposure and time since onset of exposure. Assuming that in each time-since-exposure-onset category the number of deaths from all causes is proportional to the number of person-years, an average cumulative exposure was estimated for each time-since-exposure-onset category. Similarly, using Table V in Seidman et al. (1986), which contains expected numbers of deaths from all causes cross-classified by cumulative exposure and time since onset of exposure, an average duration of exposure was estimated for each time-since-exposure-onset category. The ratio of the estimate of cumulative exposure and duration of exposure provides an estimate of the exposure intensity (f/ml) in each time-since-exposure-onset category. Using this estimate of exposure and the midpoint of the duration of exposure range for each cell, an average cumulative exposure was estimated for each cell in Table X of Siedman et al., in which lung cancer data were cross-classified using the same scheme as was used in Table V for deaths from all causes. The EPA lung cancer model (Equation 7-2) was then fit to the lung cancer mortality data in this table. This bivariate table was then collapsed by summing over cumulative exposure categories to produce Table 7-5, which categorizes the Seidman et al. (1986) lung cancer data by time-since-exposure-onset.

only 1.5 years, time since first exposure approximates time since last exposure. Because Seidman et al. (1986) did not include a lag in their exposure estimates, only data for times since first exposure >10 years are included in our analysis, since (in this range) lagged and unlagged exposures would be very similar.

Table 7-5. Fit of EPA Lung Cancer Model to Observed Lung Cancer Mortality Among New Jersey Factory Workers (Siedman et al. 1986) Categorized by Years Since First Exposure

Years Since First Exposure	Observed Deaths	Expected Deaths	Relative Risk	Predicted Deaths by Model (α=3.4)
10–14	13	8.1	1.6	16.2
15–19	20	8.8	2.3	18.8
20–24	17	9.0	1.9	20.1
25–29	22	8.6	2.5	20.8
30–34	21	6.1	3.5	17.8
35+	16	4.2	3.8	15.3
Total	109	44.7		109.0
	Goodness of Fit P-value			0.55

The RR of lung cancer increases with time since the beginning of exposure in the Seidman cohort. Nevertheless, the fit of the U.S. EPA model to these data with α estimated is very good (p=0.55) and the numbers of cancer deaths predicted by the model agree closely with the observed numbers, even up through 35+ years from the beginning of exposure. Time since last exposure (estimated in each cell as time since first exposure minus average duration of exposure) is not a significant predictor of lung cancer mortality (K is not significantly different from zero, p=0.33). The values of α (3.4) and K_L (0.01 (f-y/ml)$^{-1}$) estimated from this analysis agree closely with those estimated in Appendix A by a different approach (cf. Table A-13 in Appendix A). The analysis in Appendix A was also repeated after eliminating workers who worked longer than 2 years (i.e., workers for whom time since first exposure was not a good approximation to time since last exposure). Results obtained in this analysis are very similar to those shown in Table 7-5.

These analyses of the relationship between lung cancer mortality and time after exposure ends are based on cohorts exposed to relatively pure asbestos fiber types: crocidolite (Wittenoom, Table 7-3), chrysotile (South Carolina factory, Table 7-4) and amosite (Patterson, New Jersey factory, Table 7-5). All three of these were consistent with the assumption inherent in the U.S. EPA lung cancer model (Equation 7-2) that RR of lung cancer mortality remains constant after 10 years past the end of exposure. Thus, the U.S. EPA model appears to adequately describe the time-dependence of lung cancer mortality in asbestos exposed cohorts.

7.2.1.3 Smoking-Asbestos Interaction With Respect to Lung Cancer

The existence of an interaction between smoking and asbestos in causing lung cancer has been known for many years. For example, Hammond et al. (1979), in a study of U.S. insulation workers, found a multiplicative relationship between smoking and asbestos exposure in causing lung cancer. A multiplicative relationship for the interaction between smoking and asbestos is also the relationship inherent in the U.S. EPA lung cancer model (Equations 7-1 and 7-2), by virtue of the fact that increased risk from smoking in reflected in the background risk, which is multiplied by the asbestos-induced RR. More recent work, however, suggests that the interaction between smoking and asbestos exposure may be more complicated.

As described by Liddell (2001), many reviews of the interaction between smoking and asbestos exposure have tended to conclude that the interaction is multiplicative due primarily to (1) the conclusions of Hammond et al. (1979), which was the largest of the early studies and was thus most heavily weighted, and (2) lack of viable alternatives among the options considered. As Liddell (2001) explains, commonly, reviewers examined fits of a simple multiplicative model or a simple additive model and found that (of these two) the multiplicative model tended to provide a better fit, although the fits of either model were sometimes relatively poor. Moreover, only limited sets of mortality data from asbestos exposed cohorts could be used to evaluate these model fits because only limited smoking histories had been collected among such cohorts and, among the data sets studied, the evaluation was typically limited to distinguishing effects among dichotomous groups (i.e., non-smokers and smokers, the latter of which were treated as a single, collective group).

In a more recent analysis of cigarette smoking among the cohort of Quebec miners and millers exposed to chrysotile (which had been previously described in numerous studies, see Appendix A), Liddell and Armstrong (2002) found that the interaction between smoking and asbestos exposure was complex: certainly less than multiplicative, but not quite linear either.

To get some idea of the possible impact of a non-multiplicative asbestos-smoking interaction upon our work to reconcile lung cancer exposure-response coefficients calculated from different environments, consider the generalized model for RR,

$$RR = \delta + \beta_S \cdot S + \beta_A \cdot A + \gamma \cdot A \cdot S \qquad \text{(Eq. 7-3)}$$

where S is a measure of the amount smoked, A is a measure of asbestos exposure, and δ, β_S, β_A and γ are parameters. If $\gamma=0$, the model predicts an additive smoking/asbestos interaction, and if $\gamma=\beta_S * \beta_A / \delta$, the model becomes

$$RR = \delta * [1 + (\beta_S / \delta) \cdot S] * [1 + (\beta_A / \delta) \cdot A] \qquad \text{(Eq. 7-4)}$$

which is a multiplicative smoking/asbestos interaction. Thus, this model generalizes both additive and multiplicative interaction, and has been used by a number of researchers, including Liddell and Armstrong (2002), to study smoking/asbestos interactions.

Note that the generalized model Equation 7-4 can be written in the form

$$RR = (\delta + \beta_S * S) * [1 + A * (\beta_A + \gamma * S)/(\delta + \beta_S * S)] \qquad \text{(Eq. 7-5)}$$

Further, note that Equation 7-5 is of the form: $const_1 * (1+const_2*[\text{asbestos exposure}])$, which is the same form as the U.S. EPA lung cancer model (Equation 7-2), except that in Equation 7-5 $const_1$ ($=\delta+\beta_S*S$) and $const_2$ ($=(\beta_A+\gamma*S)/(\delta+\beta_S*S)$) depend upon the amount smoked, while in the U.S. EPA lung cancer model (Equation 7-2) $const_1$ ($=\alpha$) likewise depends upon the amount smoked, but the $const_2$ ($=K_L$) does not. Thus even with this generalized model, the U.S. EPA model would still apply, although the K_L estimated would depend upon the smoking habits of the underlying cohort. That the generalized model Equation 7-3 is at least approximately correct is supported by the fact that the U.S. EPA model (Equation 7-2), which we have noted is comparable to Equation 7-3 except that the K_L value may depend upon smoking, provided a valid fit to data from all of the 20 studies to which it was applied.

This at least suggests that, even if the multiplicative interaction assumed by the U.S. EPA model (Equation 7-2) is not correct, as long as the smoking habits in different cohorts don't differ extremely, the K_L value from different cohorts will be estimates of nearly the same quantity. In particular, the differences in the estimated K_L produced by differences in smoking habits in different cohorts is likely to be a relatively small component of the very large variation in the K_L computed from different studies (see, e.g., Table A-1 in Appendix A). In that case, K_L computed from different environments using the U.S. EPA model (Equation 7-2) would still be comparable and it would be meaningful to search for measures of asbestos exposure ("exposure indices") that better rationalize K_L values (calculated using Equation 7-2) from different studies.[3]

Although the above argument suggests that efforts to reconcile K_L values from different cohorts is still a valid and useful exercise, even if the smoking/asbestos interaction is not multiplicative, as assumed by the U.S. EPA model, further evaluation of the interaction between smoking and asbestos exposure, including evaluation of different exposure-response models, is clearly warranted. However, it must be recognized that the ability to conduct such evaluation will be limited by the small number of asbestos-related epidemiology studies in which smoking data are available, and possibly further limited by the ability to gain access to the raw data from these studies. It should also be recognized that smoking data are not available for most of the studies currently available (see, e.g., Table A-1 in Appendix A), and, for most of those studies, the published data are probably not sufficient to allow fitting of a model that incorporates any smoking/asbestos interaction other than multiplicative.

[3]However, if the interaction is not multiplicative as assumed by the EPA model, it could be problematic to use a K_L value estimated from the model to quantify absolute asbestos risk (e.g., from lifetime exposure) while taking into account smoking habits.

7.2.1.4 Conclusions Concerning the Adequacy of the U.S. EPA Lung Cancer Model

Three principle assumptions inherent to the U.S. EPA lung cancer model were considered in this study to evaluate the overall adequacy of the model for describing the manner in which asbestos exposure induces lung cancer. These are:

- that lung cancer RR is proportional to cumulative exposure (lagged 10 years);
- that risk remains constant following 10 years after the cessation of exposure; and
- that the interaction between smoking and asbestos exposure is multiplicative.

The findings from this evaluation are summarized briefly below. For convenience, timed-dependence is addressed first.

In Section 7.2.1.2, the time response predicted by the lung cancer model (Equation 7-2) was evaluated using the Wittenoom and South Carolina data, along with the data from a New Jersey amosite factory (Seidman et al. 1986). Follow-up in the Wittenoom and South Carolina was sufficient to permit evaluation of the adequacy of the model 40–45 years past the end of exposure, and follow-up in the New Jersey factory permitted the model to be evaluated up through 35+ years past the end of exposure.

The data from all three studies were consistent with the assumption inherent in the lung cancer model that RR of lung cancer mortality remains constant after 10 years past the end of exposure. That this result holds equally for a cohort exposed to chrysotile (South Carolina) as for cohorts exposed to crocidolite (Wittenoom) and amosite (New Jersey factory) is particularly noteworthy, because chrysotile fibers have been reported to be much less persistent than amphibole fibers *in vivo* (see Section 6.2.4). The fact that the lung cancer risk in South Carolina remained elevated 40–45 years following the cessation of exposure, along with the fact that the K_L from the South Carolina cohort is the largest K_L value obtained from our review of 20 studies (see Table A-1 in Appendix A) suggests that carcinogenic potency of asbestos is not strongly related to durability, at least for lung cancer (see Section 6.2).

Based on the results indicated in Section 7.2.1.1, the linear, RR exposure-response model for lung cancer (Equation 7-2) provides an adequate description of the exposure-response relationship from 20 studies. There is little evidence that exposure-response is sub-linear or "threshold-like". However, in a number of these cases the fitted model predicts a background response that is higher than that in the control population. If the background rate in the control population was actually appropriate in these studies, the exposure-response relationship in these studies would appear in some cases to be supra-linear. These results further reinforce the recommendation of the expert panel (Appendix B) that evaluation of a broader range of exposure-response models (including those that incorporate smoking-asbestos interactions that are other than multiplicative) for lung cancer is appropriate.

Although further evaluation of alternate models is warranted, the specific studies for which α=1.0 does not provide an adequate fit to the data do not appear to be related by mineral type, industry, or size of study cohort and such studies total fewer than half of the studies evaluated. Coupled with the additional evidence that the linear, RR model for lung cancer (Equation 7-2) provides a good description of the time-dependence of disease mortality during and following exposure and that it is not likely to grossly underestimate exposure despite limitation in the manner that smoking is addressed (Section 7.2.1.3), this suggests that use of this model may be adequate for estimating exposure-response factors for the existing studies, at least unless and until a model that provides a superior fit to the data is identified.

Further support for the U.S. EPA lung cancer model is also provided by Stayner et al. (1997). Stayner et al. evaluated the relative fit of a variety of additive, multiplicative, and more complex, empirical models to the same raw data from the South Carolina textile plant that we evaluated and conclusions drawn by these researchers generally parallel and reinforce those reported here.

Stayner et al. (1997) found a highly significant exposure-response relationship for lung cancer and that a linear, RR model (similar to that described by Equation 7-1, except that they initially assumed a lag of 15 years) provided the best overall fit to the data (among the additive and multiplicative models evaluated). Moreover, the fit to the data was not significantly improved by adding additional parameters, nor was there any indication of a significant interaction with any of the covariates evaluated (age, race, sex, or year). These researchers did find an interaction with time such that by applying different slopes for different latencies (15–29 years, 30–39 years, and >40 years), they were able to obtain a significantly better fit. However, Stayner et al. (1997) did not evaluate a RR model with a single slope using a lag of 10 years. Therefore, their analysis cannot be used to evaluate the effect of assuming different slopes for different latencies with respect to the U.S. EPA model, which assumes a lag of 10 years.

Because we found that mortality among the South Carolina cohort is adequately described with α=1.0, the Stayner et al. (1997) study does not directly address questions concerning supra linearity that have been suggested in our findings. Nevertheless, taken as a whole, the evidence evaluated here suggests that the model described in Equation 7-2 may be adequate for evaluating the relationship between asbestos exposure and lung cancer mortality among the existing epidemiology studies. Certainly, no clearly superior model has yet been identified. Therefore, the U.S. EPA lung cancer model was employed in this study for evaluating lung cancer risk while we also recognize that further evaluation of alternate models is warranted. The primary obstacle to more fully evaluating alternate models has been and continues to be lack of access to the raw data for a greater number of cohorts.

7.2.2 Estimating K_L values from the Published Epidemiology Studies

The U.S. EPA model for lung cancer (Equation 7-2) was applied to each of the available epidemiology data sets to obtain study-specific estimates for the lung cancer exposure-response coefficient, K_L. Based on the results presented in Section 7.2.1.4, while there is some evidence that models in addition to the U.S. EPA lung cancer model should be explored, there is little indication that the current model does not provide an adequate description of lung cancer mortality that is sufficient to support general risk assessment. The set of K_L values derived from

available epidemiology studies are presented in Table 7-6, which is a reproduction of Table A-1 in Appendix A.

In Table 7-6, Column 1 lists the fiber types for the various studies, Column 2 lists the exposure settings (industry type), and Column 3 indicates the specific locations studied. Column 4 presents the best estimate of each K_L value derived for studies, as reported in the original 1986 Health Effects Update and Column 5 presents the reference for each respective study. Columns 6, 7, and 8 present, respectively: the best-estimates for the K_L values derived in our evaluation for all of the studies currently available (including studies corresponding to those in the 1986 Health Effects Update); a statistical confidence interval for each K_L value (derived as described in Appendix A); and an uncertainty interval for each K_L value (also derived as described in Appendix A). The reference for the respective study from which the data were derived for each K_L estimate is provided in the last column of the table. To assure comparability across studies, values for all studies (even those that have not been updated since their inclusion in the 1986 Health Effects Update) were re-derived using the modified procedures described in Appendix A.

As explained in Appendix A, the uncertainty intervals for K_L values (and corresponding intervals for K_M values, the exposure-response coefficients for mesothelioma) are intended to reflect, in addition to statistical variation, other forms of uncertainty that are difficult to quantify, such as model uncertainty and uncertainty in exposure estimates. We interpret these informally as providing a range of K_L values that are reasonable, based on the data available for a given study. Accordingly, if uncertainty intervals for two K_L values do not overlap, these two underlying sets of data are considered to be incompatible. Potential reasons for such incompatibility include the possibility that the K_L values are based on an exposure measure that does not correlate well with biological activity of asbestos. One of the goals of this report is to determine an exposure index that correlates better with biological activity, and consequently brings the K_L values into closer agreement. The degree of overlap of the corresponding uncertainty intervals provides an indication of the extent to which a groups of K_L values are in agreement.

The K_L values derived in this study and the corresponding values derived in the original 1986 Health Effects Update generally agree at least to within a factor of 3; a couple vary by a factor of 4; one varies by a factor of 5; and one varies by a factor of about 15. However, in every case the K_L from the 1986 update lies within the uncertainty interval for the K_L derived in the current update.

Perhaps the most interesting of the changes between the 1986 K_L value estimates and the current K_L value estimates involves the friction products plant in Connecticut (McDonald et al. 1984). Although a relatively small, positive exposure-response was estimated from this study in the 1986 Health Effects Update, the best current estimate is that this is essentially a negative study (no excess risk attributable to asbestos). The difference derives primarily from allowing α to vary in the current analysis. The exposure groups in this cohort do not exhibit a monotonically increasing exposure-response relationship and, in fact, the highest response is observed among the group with the lowest overall exposure. As indicated in Appendix A, lack of a monotonically increasing exposure-response relationship is a problem observed in several of the studies evaluated.